Russian Chemical Reviews **70** (9) 717 – 734 (2001) © 2001 Russian Academy of Sciences and Turpion Ltd

DOI 10.1070/RC2001v070n09ABEH000675

Superconducting MgB_2 and related compounds: synthesis, properties and electronic structure

A L Ivanovskii

Contents

I.	Introduction	717
II.	Magnesium borides: a brief history of investigations (1895 – 2000)	718
III.	Magnesium diboride, a medium-T_c superconductor	720
IV.	Conclusion	730

Abstract. The discovery of superconductivity in magnesium diboride ($T_c \approx 40$ K), announced in January 2001, stimulated intensive research into the nature of superconductivity and electrophysical, magnetic and thermodynamic properties and spectroscopic characteristics of MgB_2 and related compounds. The review concerns methods for the synthesis of new MgB_2-based superconductors with more complex chemical composition. Particular emphasis is placed on the results of investigations on the electronic structure and peculiarities of chemical bonding in these compounds. Materials science aspects of practical utilisation of materials based on the new superconductor are analysed. Main results of theoretical and experimental studies in the above-mentioned fields are generalised. The bibliography includes 228 references.

I. Introduction

In his lecture at the International Symposium on Transition Metal Oxides (Sendai, South Korea, 2001) J Akimitsu announced [1] the discovery of superconductivity in MgB_2 (for more detailed information, see Ref. 2). Magnesium diboride is a relatively poorly studied representative of a broad class of metal borides.[3–14] The discovery of superconductivity in MgB_2 has immediately attracted considerable interest in this system. The transition temperature for MgB_2 ($T_c \approx 40$ K) is almost twice as high as the values of T_c for all other binary superconductors, *e.g.*, compounds and alloys with B1- (NbN, $T_c \approx 17.3$ K) or A15-type (Nb_3Ge, $T_c \approx 23$K) structures.[15,16] From the viewpoint of its properties, magnesium diboride stands apart from all known borides. For instance, the values of T_c for binary *d*-metal borides,[9,17] as well as for ternary ($LnRuB_2$, $LnRh_4B_4$) and pseudoternary [$(Ln_{1-x}Ln'_y)Rh_4B_4$] borides [18] lie between $\leqslant 0.5$ and 8 K. The highest transition temperatures ($T_c \approx 16-23$ K) were found for intermetallic borocarbides (IBC), namely, layered quaternary compounds of the $LuNi_2B_2C$ type [19–21] belonging to 'conventional' superconductors.[22]

A distinctive feature of magnesium diboride is that the value of T_c for this compound is 'intermediate' between those of classical low-temperature (LTSC) and high-temperature superconductors (HTSC). To emphasise this feature, MgB_2 is sometimes called a medium-T_c superconductor. It is of great importance that, unlike high-temperature superconducting complex oxides, MgB_2 is a non-oxygen compound with very simple chemical composition and structure.[3–8]

The discovery of superconductivity in MgB_2 has raised a number of questions.

1. What is the nature of the superconductivity in MgB_2?
2. Is magnesium diboride a unique compound of this kind or is it the first representative of a new class of superconductors?
3. What physical and chemical properties should related superconductors possess?

Answers to these questions can predetermine a breakthrough in understanding the nature of the superconductivity in crystals and physical chemistry of inorganic compounds and in outlining possible application areas of new superconductors.

In spite of short time that has elapsed since the discovery of superconductivity in MgB_2, experimentalists and theoreticians have accumulated a great body of information about its properties.

New superconductors have been found and superconducting materials based on MgB_2 were obtained in the form of powders, single crystals, films, wires and composites. It was found that the superconductivity parameters of MgB_2 remain stable in magnetic fields and upon neutron irradiation. Magnesium diboride is characterised by high critical transport currents and, at the same time, by their low sensitivity to grain boundary contacts. These and some other properties of this novel superconductor seem to be rather attractive for its practical utilisation.

The main goal of this review is to generalise a considerable body of information about magnesium diboride, its functional properties and possible application areas accumulated to date. Taking into account a great deal of interest in MgB_2, we have briefly outlined the history of investigations of the system Mg – B and reported the available data on the properties of magnesium borides. Particular emphasis is placed on the results of recent studies on the nature of the superconductivity in and physicochemical properties of MgB_2 (including the year 2001). The review concerns the results of both theoretical modelling and experimental research into the electronic structure and the nature of chemical bonding in magnesium diboride and related compounds. Problems associated with search for new superconductors based on MgB_2 and some materials science aspects are also outlined.

A L Ivanovskii Institute of Solid State Chemistry, Urals Branch of the Russian Academy of Sciences, ul. Pervomaiskaya 91, 620219 Ekaterinburg, Russian Federation. Fax (7-343) 274 44 95. Tel. (7-343) 274 53 31. E-mail: ivanovskii@ihim.uran.ru

Received 19 April 2001
Uspekhi Khimii **70** (9) 811 – 829 (2001); translated by A M Raevsky

II. Magnesium borides: a brief history of investigations (1895–2000)

Magnesium borides were first obtained by Moissan in 1895.[23] Analysis of products of the interaction between metallic magnesium and boric anhydride revealed two magnesium borides with strongly different chemical stabilities. One of the borides was found to decompose in acids to give boranes, mostly B_4H_{10}. More recently, this boride, with the chemical composition Mg_3B_2,[24–28] was studied[24] for use as starting material in the synthesis of boranes. The assumption of the existence of the second boride, Mg_2B_4 (MgB_2), was proposed[29] based on the results of analysis of boride hydrolysis products.

Studies carried out by researchers from the USSR[3,8] and other countries[4–7] over a period of two decades, from 1950s to 1970s, serve as a basis for present-day knowledge of the system Mg–B. Magnesium borides can be obtained by (i) reduction of B_2O_3 with metallic magnesium,[23] (ii) direct interaction of elemental Mg and B, (iii) reduction of MgO with boron, (iv) reduction of Na_2BF_6 with magnesium and (v) by reactions between Mg and BCl_3 and between MgO and boron carbide.[3,8] Pioneering studies on the phase equilibria in the system Mg–B and physicochemical properties of particular magnesium borides also date back to the above-mentioned two decades.

1. Phase relations in Mg–B system

No detailed phase diagram of the system Mg–B is available. Information about stable magnesium borides is contradictory (see, *e.g.*, Refs 3–13, 30). On the one hand, the occurrence of four phases (MgB_2, MgB_4, MgB_6 and MgB_{12}) is assumed.[30] On the other hand, the assumption of the occurrence of the lowest magnesium boride, Mg_3B_2, was rejected.[31] Six magnesium boride phases (MgB_2, MgB_4, MgB_6, a variable composition phase MgB_6–MgB_{17} and two phases of unknown composition) have also been reported.[32] The following phases were found in the phase diagram of the system Mg–B reported in monograph[33]: MgB_2, MgB_4 and MgB_7 (Fig. 1). Below we will consider only those magnesium borides for which reliable structural information is available.

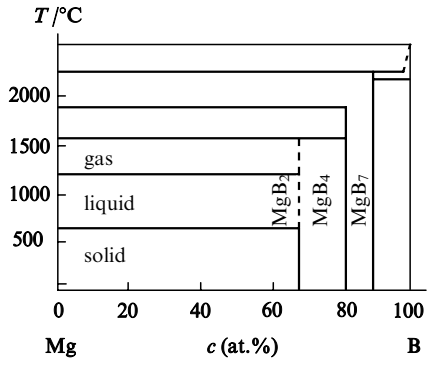


Figure 1. Phase diagram for the Mg–B system.[33]

2. Crystal chemistry of magnesium borides

Pioneering studies on the crystal structure of MgB_2 date back to the early 1950s.[34–40] Magnesium diboride has a hexagonal AlB_2-type structure. The space group is $P6/mmm$ (D^1_{6h}), the number of formula units in the unit cell $Z = 1$. Boron atoms occupy positions at the centres of trigonal prisms while magnesium atoms occupy positions at their vertices. Such prisms share all faces, thus forming a three-dimensional packing. The structure of MgB_2 can be represented as alternating planar hexagonal Mg layers and graphite-like (honeycomb) boron sheets (Fig. 2). The alternation pattern is Mg–B_2–Mg–B_2... The coordination number (CN) of magnesium atoms is 20 and their coordination polyhedron (CP) is [$MgB_{12}Mg_8$]. For boron atoms, CN = 9 and the CP is [BMg_6B_3]. The atomic positions in the unit cell are as follows: Mg, 1*a* (0,0,0) and B, 2*d* (1/3, 2/3, 1/2) and (2/3, 1/3, 1/2). The lattice constants are $a = 3.0834$ and $c = 3.5213$ Å; $c/a = 1.142$. The interatomic distances are B–B $(a/\sqrt{3}) = 1.780$, B–Mg $(\sqrt{a^2/3 + c^2/4}) = 2.503$, Mg–Mg (in-plane) = 3.083 and Mg–Mg (interlayer) = 3.520 Å.[10,38–40]

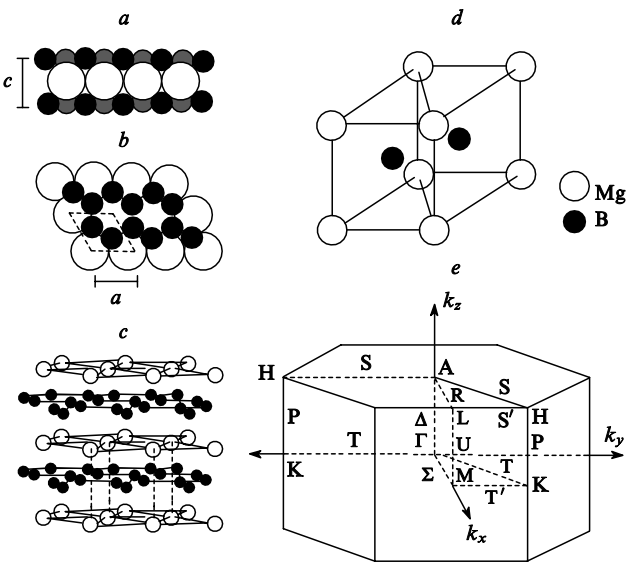


Figure 2. Structure of MgB_2.
Types of atomic packing: interlayer packing, side view (*a*); in-plane packing, top view (*b*); packing of atomic layers, side view (*c*); primitive unit cell (*d*) and the Brillouin zone (*e*).

Currently, more than a hundred of binary compounds with the AlB_2-type structure are known, including diborides of *p*- and *d*-elements.[3–13,38–40] Nevertheless, the problem of the existence of general physical or chemical criteria determining the conditions for the formation of structural types of various borides remains a moot question as yet. From the standpoint of crystal chemistry,[10] structural types of borides can be explained taking into account the ratio of atomic radii (r) of the components M/B (M is metal). According to the theory of symmetry of close crystal packings of spheres, an 'ideal' value of r_M/r_B for trigonal prismatic coordination is 1.89. For stable hexagonal MB_2 phases, the ratio r_M/r_B varies from 1.14 to 2.06[38] (*e.g.*, $r_M/r_B = 1.571$ for aluminium diboride and 1.758 for magnesium diboride).

Pearson[40] proposed an empirical criterion for the existence of AlB_2-type structures, namely, a correlation between structural parameters (c/a) of stable phases and the ratio r_M/r_X (here, X is an element whose atoms can form graphite-like sheets; in addition to boron, the set X can include Be, Si, Ga, Hg, Zn, Cd, Al, Cu, Ag and Au, see Refs 38–40). The ratio c/a varies from 0.59 to 1.2 (Fig. 3). As can be seen, the point corresponding to MgB_2 ($c/a = 1.142$) is located near the upper critical bound of structural stability. According to Pearson,[40] the occurrence of hexagonal CaB_2, which is the closest analogue of superconducting MgB_2 (see below), is impossible.

Magnesium tetraboride was first synthesised in 1953.[35] The crystal structure and properties of this compound have been studied in detail.[31,41–43] Crystals of MgB_4 belong to orthorhombic system (the space group $Pnam$, $Z = 4$) and are characterised by the unit call parameters $a = 5.464$, $b = 7.472$ and $c = 4.428$ Å.[42,43] The structural motif can be represented as pentagonal pyramids built of boron atoms, which form extended chains. Magnesium atoms occupy positions between boron polyhedra. The shortest distances are Mg–B = 2.392 and Mg–Mg = 3.075 Å. The atomic positions in the unit cell are as follows: Mg, 4*c*: x, y, 1/4 ($x = 0.051$, $y = 0.136$); $B_{1,2}$, 4*c*:

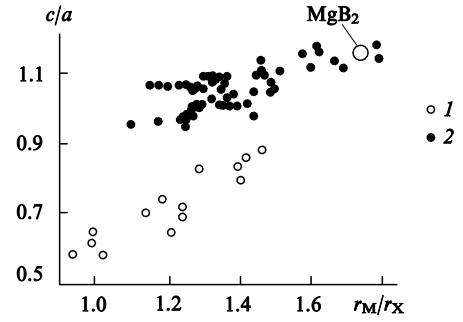


Figure 3. Dependence of the ratio of lattice parameters (c/a) on the ratio of atomic radii (r_M/r_X) for AlB_2-type binary phases MX_2;[40] c/a: <0.9 (*1*) and >0.95 (*2*).

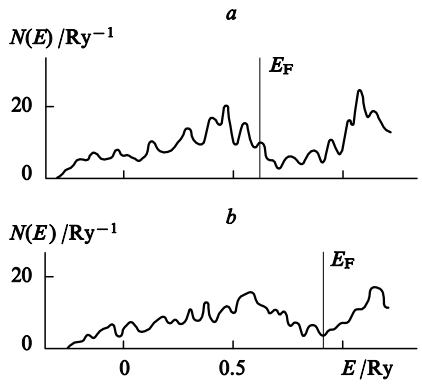


Figure 4. Total densities of states for MgB_2 (*a*) and AlB_2 (*b*) obtained from FLMTO calculations.[49]

($x_1 = 0.725$, $y_1 = 0.657$; $x_2 = 0.559$, $y_2 = 0.854$) and B_3, 8*d*: x, y, z ($x = 0.130$, $y = 0.434$, $z = 0.442$).[10] This structural type is unique in its kind since most of binary metal tetraborides [5–9, 12, 13] belong to the CrB_4 and ThB_4 structural types.

The existence of magnesium hexaboride, MgB_6, also remains a moot question as yet. It is thought that such a hexaboride represents a mixture of magnesium heptaboride MgB_7 and magnesium tetraboride MgB_4 while MgB_9 represents a mixture of MgB_7 and elemental boron.[44] The structure of magnesium heptaboride MgB_7 (Mg_2B_{14}) is characterised by a CN of 28 for the magnesium atom.[45] Similar structural elements are also inherent in $MgAlB_{14}$ ($Mg_{1-x}Al_{1+y}B_{14}$), $LiAlB_{14}$ and NaB_{15}.[10] On the other hand, MgB_7 and Mg_2B_{14} were described as individual phases with different lattice constants.[13]

3. Magnesium borides: properties, electronic structure and chemical bonding

Information about physicochemical properties of magnesium borides is scarce.[3, 8, 9, 11, 13] Only hydrolytic stability of magnesium borides and their reactions with acids have been studied in detail. It was found that boranes are formed only in the reactions with MgB_2. From the viewpoint of its reactivity and solubility in acids, this compound differs strongly from both higher magnesium borides and most of *d*-metal diborides which possess high chemical stability. Some thermochemical and thermal properties of MgB_2 (heat capacity, enthalpy, entropy and dissociation pressure, heats of formation) have been reported.[8, 9, 13]

To our knowledge, no studies on the electronic structure and the nature of chemical bonding in magnesium borides, except for MgB_2 and 'MgB_6', have been carried out so far. By analogy with other metal–boron systems, it can only be assumed that covalent B—B bonds (within boron polyhedra) should have increased importance in the overall system of interatomic interactions responsible for improvement of thermomechanical properties and chemical stability of magnesium borides on going from lower borides to higher (from MgB_2 to 'MgB_{12}').

The energy band structure of MgB_2 was studied [46–48] by the semiempirical LCAO,[47] tight binding [48] and non-self-consistent orthogonalised plane wave (OPW) methods.[46] The structures of the valence bands of MgB_2 and graphite were found to be similar.[46] The major contribution to the valence band of magnesium diboride comes from the combination of boron $p_{\sigma,\pi}$-orbitals.[47] Charge transfer occurs from Mg to B. The position of the bottom of the conduction band is determined by B boron p_π-orbitals. Comparison of the energy band structure for MgB_2 and the hypothetical crystal $\square B_2$ with 'empty' cation sublattice allowed one to draw a qualitative conclusion about the dominating role of B—B interactions in the overall system of chemical bonds.

The energy band structure as well as the chemical bonding and energy parameters of MgB_2 obtained from the first nonempirical calculations carried out by the self-consistent full-potential linear muffin-tin orbital (FLMTO) method [49] were analysed and compared with the corresponding characteristics of isostructural borides (AlB_2 and TiB_2). Among the known diborides MB_2, titanium diboride exhibits exceptionally high thermomechanical and strength properties.[7–9] The total densities of states (DOS) for MgB_2 and AlB_2 are shown in Fig. 4. The energy band structure consists of two broad bands separated by a DOS minimum (a pseudogap). A qualitative explanation for differences between the properties of MgB_2 and AlB_2 was obtained [49] in the framework of the rigid band model (RBM) [50–52] based on the structure of the valence band. According to this model, both chemical stability and thermomechanical properties of MB_2 are related to the parameter

$$V = \frac{V_b}{V_v},$$

where V_b is the width of the filled band of electron states and V_v is the total width of the valence band (up to the DOS minimum). An optimum stability corresponds to $V = 1$ (*i.e.*, all bonding bands are filled while all antibonding bands are empty). This condition holds for such *d*-metal diborides as TiB_2, ZrB_2 and HfB_2 [the valence electron concentration, VEC, is 3.33 e per atom per formula unit (see Refs 50–57)]. For MgB_2 (VEC = 2.67),[49] the calculated values are $V_v = 1.011$, $V_b = 0.912$ Ry, $V = 0.902$. For AlB_2 (VEC = 3.0 e per atom), $V_b = V_v = 1.146$ Ry, $V = 1.0$, which means that this diboride should exhibit the highest stability.

Analysis of chemical bonding in MgB_2, AlB_2 and TiB_2 using charge density maps (Fig. 5) shows that the overlap of the B—B wave functions in the plane of graphite-like sheets decreases from MgB_2 to TiB_2.[49] For TiB_2, the most pronounced is the effect of interlayer Ti—B covalent bonds, while MgB_2 is characterised by retention of spherical symmetry of the cation charge density contours. The cohesive energies (E_{coh}),† and the energies of particular (B—B, M—B and M—M) bonds were calculated (Table 1). As can be seen, the major contribution to the cohesive

† As is known, E_{coh} describes the overall effect of chemical bonding in crystals.

Table 1. Cohesive energies (E_{coh}) and energies of particular bonds (E_b) for magnesium, aluminium and titanium diboride /Ry per unit cell.[49]

Parameter	MgB_2	AlB_2	TiB_2
E_{coh}	1.26	1.42	1.58
E_b (see[a])			
M—M	0.11	0.28	0.36
B—B	0.86	0.83	0.86
M—B	0.29	0.24	0.36

[a] For calculation procedure, see Refs 53–57.

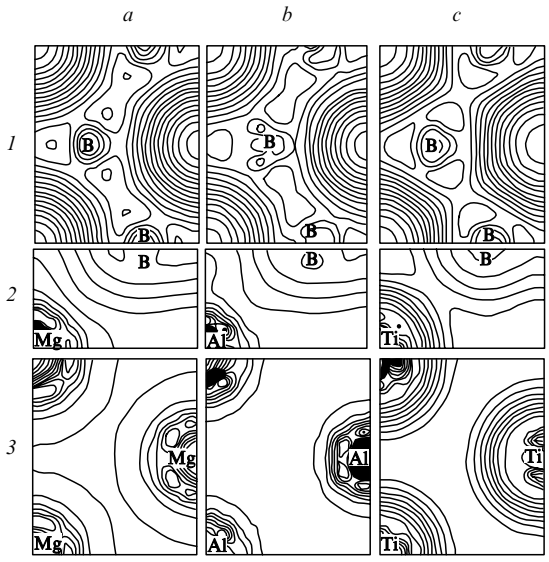


Figure 5. Charge density distributions for magnesium (*a*), aluminium (*b*) and titanium diboride (*c*): in-plane for boron sheets (*1*), in-plane for metal atom layers (*3*) and between boron sheets and metal layers (*2*).[49]

energies of MgB_2 comes from the B – B-interaction (68%). The contributions of other types of chemical bonds are much smaller (23% for B – Mg and 9% for Mg – Mg bonds). An increase in the cohesive energy on going from MgB_2 to AlB_2 is due to strengthening of the M – M bonds while the B – B and M – B binding energies vary only slightly. This is the main distinction between these compounds and *d*-metal diborides for which the value of E_{coh} depends first of all on the 'interlayer' M – B interactions.[53–57]

4. Application areas of magnesium borides

Information about application areas of magnesium borides concerns mainly MgB_2. The most attractive properties of this compound are its mechanical characteristics and high reactivity.

Magnesium diboride is used as an abrasive; polycrystalline composites based on MgB_2 and boron nitride were proposed to be used as materials for cutting devices.[13] As mentioned above, magnesium boride was used as starting material to obtain boranes following the hydrolytic decomposition reaction of the boride. Currently, the role of MgB_2 (i) as precursor in reactions of fast chemical exchange in the synthesis of refractory *d*-metal borides and ceramics based on them and (ii) in the preparation of close-packed boron nitride polymorphs has been studied intensively.

The known methods for the preparation of cubic boron nitride (c-BN), a material with record hardness, are based on heat treatment of hexagonal BN (h-BN) under pressure or precipitation from melts. Crystallisation and nucleation of c-BN are strongly affected by various catalysts, *e.g.*, C, B, Fe, Co, Ni, Cu, Al, their alloys and mixtures, as well as metal nitrides, oxides and borides.[58,59] Magnesium diboride is an efficient catalyst of spontaneous crystallisation of c-BN.[13,60–68] Studies of c-BN nucleation from melts in the system MgB_2 – BN at pressures up to 6.8 GPa and temperature up to 2000 K allowed one to determine the threshold pressure ($P \approx 4.5$ GPa) for the lower temperature bound of the c-BN phase formation ($T \approx 1630$ K).[67] The role of small additives of the third component (P, Si) on the crystallisation kinetics of c-BN in pseudoternary systems MgB_2 – BN – P (see Ref. 65) and MgB_2 – BN – Si[63,64] has been studied.

Magnesium diboride and higher magnesium borides occur among reaction products if refractory *d*-metal borides are obtained by reduction of corresponding oxides by magnesium-reduced boron

$$MO_y + B \longrightarrow MB_z + B_2O_3$$

or by magnesium reduction of such oxides

$$MO + Mg + B_2O_3 \longrightarrow MgO + MB_z.$$

At the formation temperatures of refractory borides MB_z, magnesium borides thermally decompose into boron and magnesium, the latter being removed nearly completely.[13] The procedure for preparation of dispersed ZrB_2 powders[69] is based on competitive reduction processes of ZrO_2 and boric anhydride in the system ZrO_2 – Mg – B_2O_3 (at 1100 °C) and boronation of α-Zr and Mg in the system ZrO_2 – Mg – amorphous boron (at 700 °C) followed by removal of MgO and MgB_2. A thermal reaction in the system TiO_2 – Mg – B_2O_3 in Ar atmosphere results in titanium diboride as the major product and magnesium oxide and magnesium borate ($Mg_3B_2O_6$) as side products.[70] Metal borides, solid solutions based on them and boride ceramics can also be synthesised by solid-state reactions of fast chemical exchange with participation of MgB_2.[71–73] A mechanochemical reaction in a Ti – 4% MgB_2 mixture, resulting in a nanocrystalline Ti matrix with inclusion of MgB_2 grains of size 20 to 300 nm has been studied.[74] Subsequent sintering of the reaction product at 600 °C resulted in a new compound with NiAs-type structure and unknown composition.

Along with TiB_2, B_4C, CrB_2, BN and amorphous boron, MgB_2 was announced to be an antioxidant, *i.e.*, an additive to carbon-containing refractory materials used in metallurgy to prevent them from breakdown upon oxidation of carbon in the surface layer.[75] Oxidation and phase formation in the mixture of MgB_2 synthesised in the reaction $MgB_{12} + Mg \rightarrow MgB_2$ with periclase – carbon composite have been studied as functions of temperature.[75] The process is characterised by exothermic effects, begins at ~470 °C and results in MgO, $Mg_2B_2O_5$ and boric anhydride. Similar magnesium polyborides (mixtures of amorphous boron and MgB_{12} obtained by magnesium reduction of B_2O_3) were found to behave similarly. According to DTA, the mass increased by 43%. Amorphous boron of purity 95% to 98% exhibited the best antioxidant properties; in this case, a mass increase of 124% to 147%.

The results of applied research on the use of MgB_2 as a catalyst in the synthesis of c-BN,[76] as antioxidant additive to refractory materials[77–79] and for production of dispersed alloys[80] and SiC powders (see Ref. 81) were patented.

Prospects for practical utilisation of superconducting MgB_2 will be considered below.

III. Magnesium diboride, a medium-T_c superconductor

The discovery[1,2] of superconductivity in MgB_2 and publication of pioneering studies,[82–87] in which the nature of the effect was rationalised in the framework of electron – phonon mechanism of superconductivity, has stimulated discussion about possible analogues of superconducting magnesium diboride. Both chemical composition and crystal structure aspects of the problem were considered and some other factors responsible for superconductivity were analysed. Chemical analogues of MgB_2, that is, binary and multicomponent borides, have been considered in the preceding Section of this review.

Considerable attention has been given to the role of quasi-two-dimensional (quasi-2D) structure of magnesium diboride. It has been generally thought that high lattice symmetry (preferably, cubic) is favourable for superconductivity. This can be exemplified by elemental superconductors (Nb, La under pressure and fullerite C_{60} with the transition temperatures of 9, 13 and 33 K, respectively), binary compounds (ZrN, NbN and Nb_3Ge with T_c of 10.7, 18 and 23 K, respectively) and a number of ternary compounds.[88–90]

Recently, a group of 2D-HTSC has been found. Oxides with CuO_2 layers in their structures can serve as the best known

example of these compounds. Quasi-2D β-nitrides ZrNCl (T_c = 15 K) and HfNCl (T_c = 25 K) also represent layered structures with alternating (Zr, Hf)–N and chlorine layers. Interlayer interactions in these compounds are weak and superconductivity is observed upon intercalation with alkali metal atoms.[91–93] A possible mechanism of superconductivity in anisotropic media taking into account the quasi-2D character of the energy bands has been discussed.[94]

Special attention has been given [87] to similarity in the atomic structure and electronic properties of MgB_2 and graphite. Both compounds are isoelectronic [the ionic formula of magnesium boride is $Mg^{2+}(B_2)^-$], have layered structures and exhibit a similar type of chemical bonding with strong in-plane σ-bonds and weak interlayer π-bonds. Moreover, electron-doped intercalated graphites (*e.g.*, LiC_8 and KC_8) are superconductors (up to T_c = 5 K).[95,96] There is also evidence [97] for substantial enhancement of superconductivity in specially treated fullerite C_{60} to $T_c \sim 52$ K (*cf.* $T_c \leqslant 33$ K for the known medium-T_c superconductors based on M_3C_{60}, where M is an alkali metal), which points to potentially significant role of intercalation.

The nature of these analogies can be understood by analysing the band structure and phonon spectrum of magnesium diboride. Before considering them, let us discuss methods for the synthesis of MgB_2.

1. Synthesis and properties of superconducting MgB_2

a. Synthesis of MgB_2

Currently, superconducting MgB_2 is mainly obtained as polycrystals by solid-phase synthesis from elemental B and Mg.[1,2,82–84,98–120] Synthetic procedures differ from one another in composition of starting materials, atmosphere, and heat treatment regimes. For instance, MgB_2 samples were synthesised [84] from magnesium flakes and sub-micron powder of amorphous boron which were pressed in pellets, placed on Ta foil and subsequently fired in a tube furnace under inert atmosphere (95% Ar + 5% H_2) at 600 (1 h), 800 (1 h) and 900 °C (1 h) and then lightly ground. The resulting powders were hot pressed (10 kbar, 650–800 °C) for periods between 1 and 5.5 h. The samples thus obtained were characterised by multiphase composition; however, they exhibited high critical currents.

Other sintering conditions are listed in Table 2. For instance, $Mg(^{11}B)_2$ was prepared [101] from a boron powder enriched with ^{11}B and Mg lumps placed in a BN crucible and heat-treated for 1.5 h in Ar atmosphere (P = 50 bar). No chemical composition of the sample obtained was reported. The superconductivity parameters were T_c = 39 K and the width of the transition ΔT_c = 0.4 K. Magnesium diboride samples were also synthesised [82] from a Mg : B = 2 : 1 mixture in a Ta tube placed in a quartz ampoule in Ar atmosphere. The mixture was heated to 950 °C and kept 2 h at this temperature. The procedure proposed by Gerashenko *et al.*[99] involved pressing of magnesium and amorphous boron into pellets which were placed in a Ta crucible and then subjected to two-step annealing in purified helium flow. At first, the pellets were annealed at 800 °C for 1 h. The resulting phase contained MgB_2 (78.6%), Mg (16.6%), MgO (4.7%) and BN (traces). Subsequent annealing at 875 °C (1 h) led to evaporation of the unreacted metallic magnesium. The final phase was composed of MgB_2 (89.9%), MgO (5.2%) and BN (1.7%) and characterised by T_c = 39.5 K and ΔT_c = 2.5 K. Thus, superconducting magnesium diboride powders can be obtained using rather simple synthetic procedures which do not require costly starting materials and equipment.

b. Physicochemical properties of superconducting MgB_2

The mechanism of superconductivity in MgB_2 was elucidated by measuring the isotope effect on $Mg(^{10}B)_2$ and $Mg(^{11}B)_2$ powders.[82] Replacement of ^{10}B by the heavier isotope, ^{11}B, led to a decrease in T_c from 40.2 to 39.2 K and to narrowing of the transition region by 0.1 K (Fig. 6). The isotope coefficient,

$$\alpha_B = -\frac{\Delta \ln T_c}{\Delta \ln M_B},$$

where M_B is the magnetisation of the boron sublattice, was found to be ~ 0.26. This is close to the α_B values for IBC,[105,106] the superconductivity of which is due to electron–phonon interaction (with high-frequency optical B A_{1g} modes) and is described in the framework of the Bardeen–Cooper–Schrieffer (BCS) model.[22]

Experiments with different samples [102,107,108] revealed rather high critical current densities (j_c) ($2 \times 10^4 - 10^5$ A cm^{-2}). It was found that the temperature dependences of the critical fields H_{c2} and H_{c1} near T_c have a slope of 0.012 T K^{-1} and that the magnetisation curves are reversible.[107,108] The H_{c2} anisotropy (1.73) was first measured [108] on aligned crystallite samples. The temperature dependence $H_{c1}(T)$ was reported to be linear for the whole temperature region in which superconductivity is observed.[109] At $T > T_c$, the temperature dependence of the resistivity has the form [110]

Table 2. Conditions for the synthesis of superconducting MgB_2 powders.

Atmosphere (sheath)	Sintering conditions		Phase composition	Lattice parameters /Å		T_c /K	Ref.
	T /°C	time /h		a	c		
92% Ar + 8% H_2 (Ta foil)	600 + 800 + 950, after compaction	2 + 2 + 1,	MgB_2 + MgO (impurity)	3.0815(6)	3.5191(7)	37	100
	950	2					
Inert atmosphere (a Ta tube placed in a quartz ampoule)	950	2	$Mg(^{10}B)_2$	3.1432 ± 0.03	3.5193 ± 0.03	40.2	82
Ar (Ta crucible)	850	2	$Mg(^{11}B)_2$	–	–	39.2	98
Inert atmosphere (a BN crucible on Ta foil placed in a quartz ampoule)	900, after compaction	4	single-phase $Mg(^{11}B)_2$	–	–	39	101
	1000	6					
Ar (a Ta tube in a quartz ampoule)	1200	1	–	–	3.518	–	102
MgB_2 (AA) [a]	500	72	MgB_2 + impurities (10^{-2} at.% Ni, Cu, W)	–	–	–	103
Ar (Nb tube)	900	1–3	–	–	–	–	104

[a] Commercially sold MgB_2 powder [Alfa Aesar Co, USA, assay (purity 98%)].

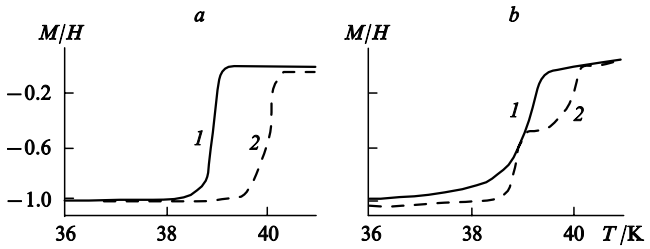


Figure 6. Isotope effect in magnesium diboride.[82]
(*a*) Magnetisation divided by magnetic field strength (M/H) as function of temperature for $Mg(^{11}B)_2$ (*1*) and $Mg(^{10}B)_2$ (*2*); (*b*) the same for $Mg(^{10}B)(^{11}B)$ (*1*) and sum of $Mg(^{11}B)_2$ and $Mg(^{10}B)_2$ data (*2*).

$$\rho(T) \approx T^2.$$

It was found that magnetic field has no effect on ρ. The Hall coefficient[111] R_H of magnesium diboride is positive (4.1×10^{-11} m^3 deg^{-1} at 100 K and a hole concentration, n, of 1.5×10^{23} cm^{-3}) and increases in the temperature range from 40 to 300 K.

An important distinction of superconducting MgB_2 from cuprate HTSC has been pointed out.[84] Due to high anisotropy, cuprate HTSC rapidly lose their performance in external fields, while the supercurrents flowing throughout even untextured, multiphase MgB_2 samples are little sensitive to weak magnetic fields. The spin–lattice relaxation rate[99,112] and the Knight shift[99] were measured by NMR spectroscopy; the behaviour of the former parameter was interpreted within the framework of *s*-wave model in the strong electron–phonon coupling limit.[112]

Magnesium diboride was also studied by the scanning tunnelling microscopy.[113–115] Particular attention was paid to the current-*vs*.-voltage characteristics used for the determination of the width of the superconducting energy gap (Δ). Large scatter of the gap widths Δ (from 5 to 7 meV, see Refs 113–115) was first of all explained by different compositions of the samples studied. The gap widths Δ were also evaluated from the tunnelling spectra of Au/MgB_2 point-contact tunnel junctions[116] (Δ = 4.3 meV) and IR reflectance spectra[117] (Δ = 4.5 meV).

The specific heat of magnesium diboride and its dependences on the magnetic field and temperature were measured,[118,119] as well as some other thermodynamic and mechanical characteristics [*e.g.*, the elasticity modulus $B_0 = 151 \pm 5$ GPa (see Ref. 120)].

The possibility of self-consistent interpretation of the results of the above-mentioned experiments in the framework of the model of electron–phonon mechanism of superconductivity in magnesium diboride[82,85–87] should be emphasised. On the other hand, Hirsch[121] proposed a 'universal' model of 'hole superconductivity' in MgB_2,[122] which implies pairing of spin carriers driven by the Coulomb interaction. However, the results obtained upon treatment of MgB_2 according to Hirsch[121] in order to increase T_c (*e.g.*, by doping with aluminium or by hydrostatic lattice compression) contradict the conclusions reported in theoretical studies based on the electron–phonon mechanism of superconductivity.

2. Electronic structure and superconductivity of MgB_2

According to McMillan,[123] the critical temperature in crystals with electron–phonon mechanism of superconductivity can be determined using the formula

$$T_c \approx \langle\omega\rangle \exp[f(\lambda)],$$

where $\langle\omega\rangle$ is the averaged phonon frequency (which is inversely proportional to the masses of the atoms), λ is the electron–phonon coupling constant [$\lambda \approx N(E_F)\langle I^2\rangle$], $N(E_F)$ is the density of states (DOS) at the Fermi level and $\langle I^2\rangle$ is the electron–ion matrix element determined by the bond ionicity. Information about the electronic structure and vibrational states of MgB_2 is of crucial importance for correct interpretation of superconductivity in and other properties of MgB_2 as well as for targeted search for new superconductors.

a. Electronic structure

The discovery of superconductivity in MgB_2 stimulated intensive theoretical[85–87,124–130] and experimental[131–133] studies of the electronic structure of magnesium diboride[85–87,124–133] and a large number of stable and metastable isostructural diborides of Li, Na,[87,125,126] Be, Ca,[124] Al,[124,126] Sc, Y, Ti, V,[124,134] Ag and Au,[127] as well as some related phases [MgB_6, CaB_6,[128] $CaSi_2$, CaSiBe,[125] $ZrBe_2$, $HfBe_2$, $CaGa_2$,[127] Mg_3BN_3 (see Ref. 129)]. Calculations were carried out using rigorous, self-consistent density functional approach.

The valence band structure of MgB_2 is determined[85–87,124–126] by the B $2p$ states which form four $\sigma(2p_{x,y})$-bands and two $\pi(2p_z)$-bands (Fig. 7). They exhibit strongly different dispersion $E(k)$. For the B $2p_{x,y}$-bands, the dispersion $E(k)$ is maximum along the $k_{x,y}$ direction (Γ–K). These bands reflect the distribution of the B states within graphite-like sheets, which have a quasi-2D type and form flat zones along the k_z direction (Γ–A). Two B $2p_{x,y}$-bands cross the Fermi level and contribute largely to the total density of states at the Fermi level [$\sim$30% (see Ref. 85)]. These bands are responsible for the metal-like properties of magnesium diboride. The Fermi level is located in the region of bonding states. Magnesium diboride exhibits hole-type conductivity, which is consistent with the results of Hall coefficient measurements.[111] Charge transfer occurs from magnesium to boron.

One of the most distinctive features[85–87,124–130] of the electronic structure of MgB_2 is the position of the B $2p_{x,y}$ energy bands. Namely, they are above the E_F at the Γ point of the

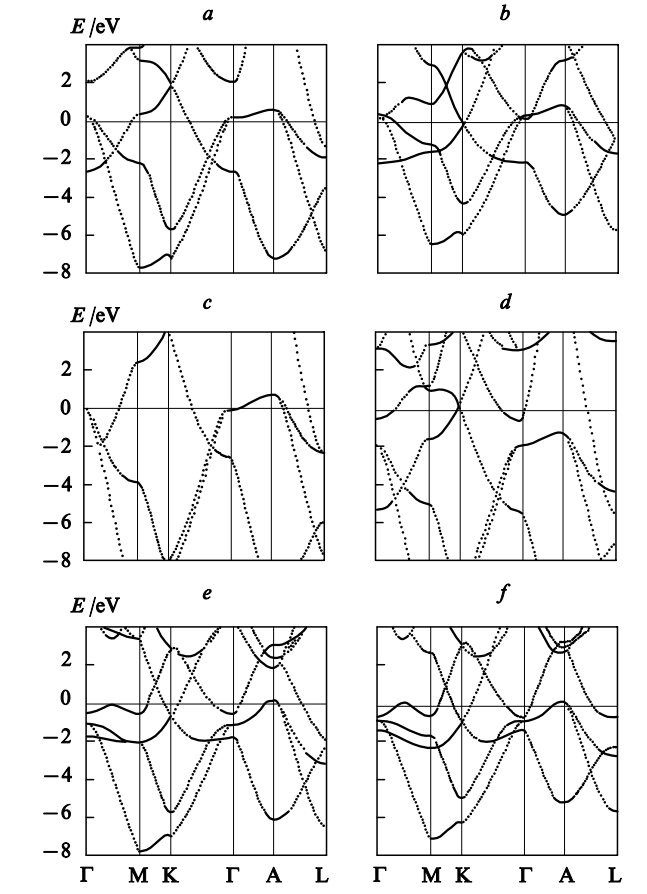


Figure 7. Energy band structures for MgB_2 (*a*), CaB_2 (*b*), BeB_2 (*c*), AlB_2 (*d*), ScB_2 (*e*) and YB_2 (*f*).[124]

Brillouin zone and form two hole-type cylinders on the Fermi surface.[85–87] The B $2p_z$-like states have a 3D-type, are oriented perpendicular to the boron sheets and are responsible for weak interlayer π bonds.[85–87, 124–126] Both π-bands cross the Fermi level and are characterised by the maximum dispersion along the k_z direction (Γ – A). The Mg *s*, *p*-states and B *s*-states are mixed with the system of B 2*p*-like bands near the valence band edge and in the conduction band. The determining role of boron in the formation of the electronic structure of MgB_2 has been particularly emphasised by Kortus *et al.*[85] who titled their communication 'Superconductivity of metallic boron in MgB_2'.

The electronic structure of magnesium diboride was studied by X-ray emission spectroscopy (XES),[131, 132] X-ray absorption spectroscopy (XAS)[131, 132] and photoemission spectroscopy (XPS).[131, 133] Comparison of the C K_α XES lines ($1s \rightarrow 2p$-transitions) for graphite and corresponding B K_α lines for MgB_2 and AlB_2 (Fig. 8) clearly demonstrates differences in positions of their emission maxima determined by the p_{xy}-states.[135] This supports the idea[85–87, 124–130] of correlation of the superconductivity in MgB_2 with the relative positions of the σ- and π-bands (the presence of hole-type σ-states). The results of XES and XAS studies[132] of the structure of B bands near the Fermi level are in excellent agreement with the results of calculations (Fig. 9). The spectra exhibit a number of resonance lines indicating the presence of a protective oxide film formed on the sample surface upon exposure to air.

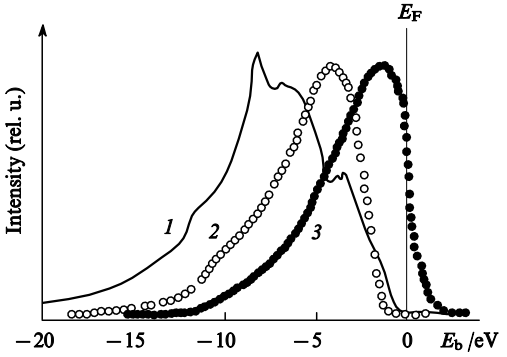


Figure 8. X-Ray emission C K_α spectra ($1s \rightarrow 2p$-transitions) for graphite (*1*) and corresponding B K_α spectra for AlB_2 (*2*) and MgB_2 (*3*).[131]

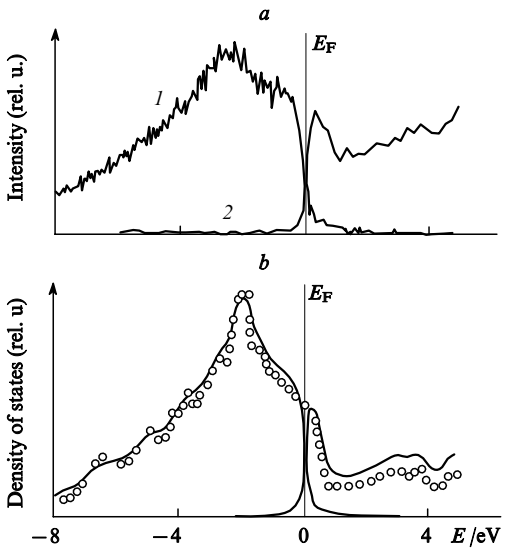


Figure 9. X-Ray emission (*1*) and absorption (*2*) spectra of boron in MgB_2 (*a*) and the DOS distribution for boron (*b*): theoretical (solid lines) and corrected for the lifetime of excited state, thermal and instrumental broadening of the experimental setup (points).[132]

High-resolution XPS studies of magnesium diboride allowed direct observation[133] of the superconducting energy gap (~4.5 meV at 15 K). This gap (~3 meV at $T = 0$ K) is of the *s*-wave character and its temperature dependence is consistent with the BCS theory.

Band structure calculations were carried out for magnesium diboride and isostructural diborides of Li, Na,[87, 126] Be, Ca,[124] Al,[124, 126] Sc, Y, Ti, V,[124, 134] Ag and Au (see Ref. 127). The band structures are compared in Figs 7 and 10. The absence of superconductivity in BeB_2 (see Ref. 136) was assumed[124] to be due to the low-energy shift of σ-bands and the absence of hole states at the Γ point, which changes the Fermi surface topology in such a manner that cylinders (along the Γ – A directions) are transformed into cones. The absence of superconductivity in AlB_2 is due to filling of σ-bands caused by the VEC increase.[83] Variations of superconducting properties for a number of *d*-metal diborides can be rationalised based on the results of calculations.[53–55, 124, 134] For ScB_2 and YB_2, the 2D-p_{xy}-bands at the A point are above the E_F (see Fig. 7), but the concentration of hole carriers is low. It is important that metal *d*-states contribute largely to $N(E_F)$. As a result, these diborides are characterised by low T_c (1.5 – 2.0 K).[9, 17] Among hexagonal transition metal diborides, the lowest T_c values should be exhibited by TiB_2, ZrB_2 and HfB_2, for which the Fermi level is located in the pseudogap.[50–55] As electron concentration increases, the *d*-band is filled and $N(E_F)$ increases[50, 52–55] (*e.g.*, for Group V and VI *d*-metal diborides). This can lead to an increase in T_c; *e.g.*, a rather high $T_c \sim 9$ K was reported for TaB_2.[137]

Analysis of the energy band structures of metastable diborides of Li, Na,[87, 126] Ca,[124] Al,[124, 126] Ag and Au (see Ref. 127) showed that the σ- and π-band configurations and band filling types

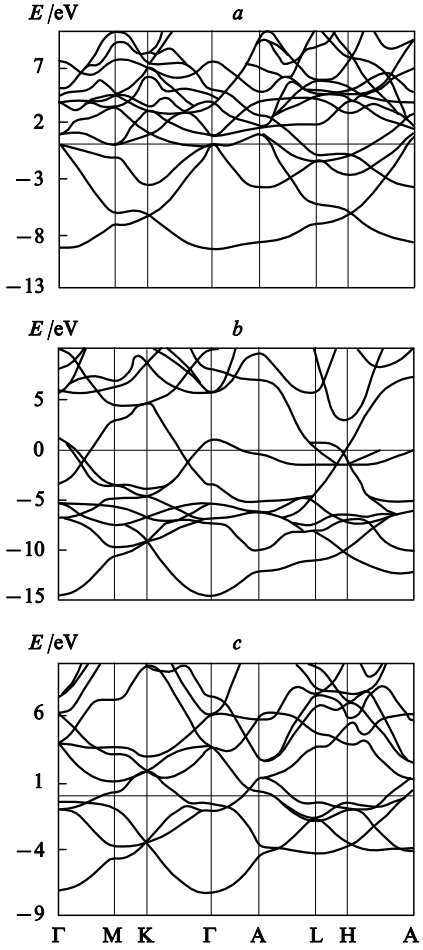


Figure 10. Energy band structures for $CaGa_2$ (*a*), AgB_2 (*b*) and $ZrBe_2$ (*c*).[127]

calculated for CaB_2 are the same as the 'optimum' parameters of superconducting MgB_2. Calcium diboride was suggested [124] to be the most probable new superconductor. Estimates [124] of the enthalpy of formation of CaB_2 (-0.12 eV per formula unit) showed the possibility of real synthesis of this compound. It is thought that calcium diboride can be stabilised by, *e.g.*, doping with isoelectronic or hole dopants (Mg, Li, Na) or by forming layered superstructures, *e.g.*, $Ca-B_2-Mg-B_2-Ca$. The electronic properties of ternary systems based on MgB_2 will be considered in the next Section of this review. Here, we will only mention that an increase in the unit cell volume will assist the formation of the electronic structure of diborides in a manner favourable for superconductivity. This can be done by, *e.g.*, isoelectronic replacement of magnesium by cations with larger atomic radii (Ca, Sr, Ba).[124]

Structural similarity between MgB_2 and hexagonal BN has been pointed out.[129] Like MgB_2, boron nitride also contains planar boron sheets while its structural stability is due to strong in-plane covalent bonds.[14, 138] The energy band structures of MgB_2 and solid solutions of composition $MgB_{2-y}N_y$, where boron was partially replaced by nitrogen, were compared.[129] Solid solutions with $y = 0.25$ and 1.00 were studied. The solution $MgB_{1.0}N_{1.0}$ (in which the composition of the non-metal sublattice formally matches the composition BN) can be considered as a model of magnesium boronitride prepared by intercalating atomic h-BN sheets with hexagonal magnesium layers. The energy band structure of the individual ternary phase Mg_3BN_3 with separated layers of different-type metalloids (B and N) was calculated.[139]

An increase in the N/B ratio in the composition of solid solutions leads to a shift of the Fermi level towards higher values, filling of antibonding states and a decrease in $N(E_F)$. The bonding B $p_{x,y}$-like bands become completely filled while the hole states are absent. According to calculations,[129] Mg_3BN_3 is a semiconductor [transition at the Γ point of the Brillouin zone, the forbidden gap (FG) width is 0.88 eV (0.065 Ry)]. The valence band structures of MgB_2 and Mg_3BN_3 are fundamentally different, *viz.*, the determining role in the mechanism of superconductivity in MgB_2 is played by the B 2*p*-bands while for Mg_3BN_3 these bands lie much below E_F and contribute negligibly to the region of the spectrum near the Fermi level.

The energy band structure of metastable cubic magnesium hexaboride (the space group *Pm*3*m*) has been studied.[140] The optimised lattice parameter corresponded to $a = 4.115$ Å. The main building blocks of the MgB_6 structure are B_6 octahedra. The energy band structure contains 10 valence bands of hybrid B 2*s*,*p*-states, which are responsible for B—B bonds both within and between B_6 octahedra. The upper filled band forms a flat zone along the $X-\Gamma$ direction and is composed of B $p_{x,y}$-orbitals involved in B—B interactions between B_6 octahedra. The first unfilled band is characterised by strong *k*-dispersion and is composed of contributions of cation states. Unlike CaB_6 (FG ≈ 0.0163 Ry, direct transition at the Γ point), magnesium hexaboride is a narrow-gap semiconductor with indirect transition (FG ≈ 0.0150 Ry, $X \rightarrow R$ transition).[10, 141–144] Despite the determining role of B—B bonds in MgB_2 and MgB_6 crystals, they possess basically different electronic properties that is, metallic for MgB_2 and semiconducting for MgB_6.

'Non-boride' AlB_2-type phases with silicon, beryllium or gallium graphite-like sheets have been reported [$CaSi_2$, CaSiBe,[125] $ZrBe_2$, $HfBe_2$, $CaGa_2$ (see Ref. 127)].

Rhombohedral $CaSi_2$ (the space group *R*3*m*) obtained under equilibrium conditions is known to be a nonsuperconducting semimetal.[145] Heat treatment of $CaSi_2$ under pressure can cause a polymorphous transformation into an AlB_2-type structure.[146] Similarity between the energy band structure of this disilicide and those of *sp*-element diborides and $CaGa_2$ (see Fig. 10)[127,146] was found.[125] The main distinctions are due to Ca *d*-orbitals which are mixed with the Si states near the bottom of the conduction band due to hybridisation. The antibonding π^*-bands are partly filled, which can be the reason for structural instability of the high-pressure phase under normal conditions. Stabilisation of hexagonal $CaSi_2$ by replacement of Si by Be was studied taking calculations of a model phase CaSiBe as an example. It was assumed [125] that (i) replacement of Si by an atom of smaller radius (*cf.* $r_{Si} = 1.34$ and $r_{Be} = 1.13$ Å) will produce 'chemical pressure', which is favourable for stabilisation of the AlB_2-type structure, and (ii) partial depletion of the π^*-band with a decrease in the electron concentration in the system will an additional stabilising factor. As was found, stabilisation of the AlB_2-type structure requires the reduction of the VEC in the system by ~ 0.7 e.[125] The electronic properties of $HfBe_2$ and $ZrBe_2$ are fundamentally different from those of superconducting MgB_2 (see Fig. 10).

b. Electronic structure and properties of superconducting MgB_2

Some properties of MgB_2 were explained using information about its electronic structure obtained from calculations. Kortus *et al.*[85] estimated the constant λ (~ 1) and phonon frequencies ($300-700$ cm^{-1}) and calculated the T_c value within the rigid atom sphere model. Their results were found to be consistent with the experiment.[2] The *ab initio* approach was also successfully used in phonon spectrum calculations, simulation of the effect of heat treatment on superconductivity in magnesium diboride and calculations of its elasitc characteristics (see below). Calculations [134] of the electric field gradients (EFG) reflect asphericity of the electron density distribution in the vicinity of atomic nuclei and are closely related to the symmetry of their nearest environment, electronic structure and the nature of chemical bonding.

Experimental EFG values are obtained in studies of quadrupole effects in the NMR spectra of MgB_2 (see Refs 99, 112) and some other diborides.[147] Analysis of the nature and regularities of variations of the EFG depending on the energy band structure of several diborides MB_2 (M = Be, Mg, Al, Sc, Ti, V, Cr) has been reported.[134] The results are listed in Table 3. Among *sp*-metal borides, BeB_2 is characterised by the largest V_{zz} component of the EFG. For 3*d*-metal diborides, the V_{zz} component changes nonmonotonically, with a minimum for TiB_2. These changes were explained [134] based on results of band structure calculations for these phases (see Fig. 7). For boron nuclei, the EFG characterises the anisotropy of partial charge density distributions

$$V_{zz} \approx \frac{p_z - (p_x + p_y)}{2},$$

where p_z, p_x and p_y are the corresponding band populations.

Table 3. EFG components on boron nuclei in borides.

Diboride	10^{-21} V_{zz} /V m^{-2}		
	FLMTO [134]	FLAPW [148] (see [a])	experiment [147]
MgB_2	1.88	—	1.69
BeB_2	2.10	—	—
AlB_2	0.99	—	1.08
ScB_2	0.60	—	—
TiB_2	0.35	0.38	0.37
VB_2	0.38	0.39	0.43
CrB_2	0.59	0.60	0.63

[a] Full-potential linearised augmented plane wave method.

According to calculations, diborides with partially unfilled p_{xy}-bands (BeB_2, MgB_2) are characterised by the largest EFG. Additional increase in EFG for BeB_2 depends on the mutual position of the p_{xy}- and p_z-bands and is determined by an increase in the population of the latter. The increase in V_{zz} in order $TiB_2 \rightarrow VB_2 \rightarrow CrB_2$ is due to fundamentally different reasons, namely, weakening of the interlayer hybrid $p-d$ metal—boron

bonds affecting the relative position and populations of the B p_{xy}- and p_z-bands.[124] Estimation of changes in the EFG on magnesium and boron nuclei in MgB_2 with pressure (up to $P = 10$ GPa) showed that an increase in pressure has little effect on the EFG at boron nuclei, whereas the EFG at magnesium nuclei rapidly increases.[134]

c. Phonon spectrum and electron – phonon interaction

Preliminary estimation of phonon frequencies obtained from band structure calculations showed [85, 87, 149] that they were consistent with the observed T_c. The authors of pioneering studies [85, 87] reported only particular modes responsible for electron – phonon coupling. The results of phonon spectrum calculations [149–151] point to the dominating role of optical phonons in the electron – phonon interaction. Similarly to electron states of the σ-bands, these optical phonons are of quasi-2D type (along the Γ – A direction of the Brillouin zone) and correspond to the in-plane vibrational modes. An important distinction between the phonon characteristics of MgB_2 and AlB_2 (Fig. 11) consists in 'softening' of the high-frequency vibrational modes in magnesium diboride and their strong coupling ($\lambda \approx 0.75$) with electrons near the Fermi level.[150] Nonsuperconducting AlB_2 is characterised by a much smaller constant λ (0.4).[150] Inelastic neutron scattering studies [101] revealed four peaks of the generalised density of phonon states, the maximum energy of atomic oscillations was found to be higher than 90 meV. The maximum energy of acoustic phonons (36 meV) was determined from analogous experiments [98] and it was shown that optical modes are characterised by strong dispersion and form peaks at 54, 78, 89 and 97 meV. The estimate [98] of the constant λ ($\lambda \approx 0.9$) obtained using the Born – von Karman model [98] is consistent with the results of calculations by Andersen *et al.*[149]

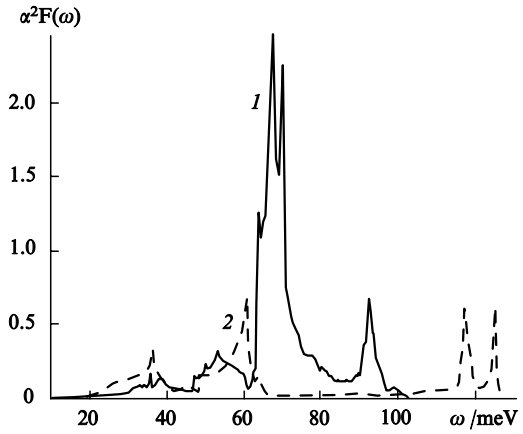


Figure 11. Eliashberg functions [$\alpha^2F(\omega)$] for MgB_2 (*1*) and AlB_2 (*2*).[150]

3. Search for new superconductors based on MgB_2 and related phases: theory and experiment

The discovery of superconductivity in MgB_2 stimulated intensive theoretical and experimental search for new related superconductors. A general trend has been to extend the variety of possible MgB_2-based superconductors by varying their chemical compositions.

a. Theoretical studies

The possibility of chemical modification of the electronic structure of 'ideal' MgB_2 by varying its chemical composition was systematically studied by the FLMTO method in the framework of supercell approach.[124, 152] The effects analysed were those produced on the band structure of MgB_2 by doping the boron sublattice with Be, C, N and O, by doping the magnesium sublattice with Be, Ca, Li, Na, Zn and Cu and by changing the diboride composition due to addition of lattice vacancies in Mg- and B-sublattices (nonstoichiometry effects). The compositions of compounds studied are listed in Table 4.

Table 4. Results of FLMTO calculations of the DOS at the Fermi level [state per (eV per formula unit)] for magnesium diboride and related binary and ternary systems.[124]

Diboride	$N(E_F)$	Diboride	$N(E_F)$
MgB_2	0.73	$Mg_{0.75}Li_{0.75}B_2$	0.73
CaB_2	0.92	$Mg_{0.50}Li_{0.50}B_2$	0.75
BeB_2	0.47	$Mg_{0.75}Na_{0.75}B_2$	0.73
$MgB_{1.75}C_{0.25}$	0.56	$Mg_{0.50}Na_{0.50}B_2$	0.76
$MgB_{1.75}$	0.61	$Mg_{0.75}Cu_{0.25}B_2$	0.89
$Mg_{0.75}B_2$	0.74	$Mg_{0.75}Be_{0.25}B_2$	0.62
		$Mg_{0.75}Zn_{0.25}B_2$	0.51

Qualitative changes in the energy band structures of solid solutions have been discussed in the framework of the RBM model.[152] It was found that dopants can act as hetero- or isoelectronic impurities which change or have no effect on the VEC in the system, respectively. According to calculations, Be impurity in the boron sublattice, Li, Na and Cu impurities in the magnesium sublattice as well as both types of lattice vacancies ('hole dopants') will, first, decrease the VEC in the system, thus leading to an increase in the concentration of hole states in the σ-band and, second, assist a shift of the E_F towards high energies with an increase in $N(E_F)$. Both these factors are favourable for superconductivity (see above). On the contrary, Al impurity in the magnesium sublattice, C, N and O impurity in the boron sublattice ('electron dopants'), will deteriorate the superconducting properties of the system due to filling of the σ-band and reduction of $N(E_F)$. In the framework of the RBM model, the role of isoelectronic replacement of Mg by Be or Ca remains unclear as yet. One can only assume that the main effects will be associated with structural factors, that is, magnesium diboride lattice distortion depending on the ratio of radii of 'host' and 'guest' elements.

Numerical calculations [124, 152] give a more complex picture (see Table 4 and Figs 12, 13). The addition of vacancies to boron sublattice ($MgB_{1.75}$) leads to a decrease in $N(E_F)$. In the series of solid solutions $MgB_{1.75}C_{0.25} < MgB_{1.75}N_{0.25} < MgB_{1.75}O_{0.25}$ the $N(E_F)$ increases nonmonotonically. This is due to the filling of antibonding states. The σ-band becomes fully occupied. It was concluded that there is no prospect for obtaining superconductivity in the system by doping the boron sublattice.[124] Based on consideration of particular binding energies (see Table 1), it was suggested that insertion of impurity into the boron sublattice is much less probable than substitution in the cation sublattice. In the latter case, the energy band structures of solid solutions $Mg_{1-x}M_xB_2$ (M = Be, Ca, Li, Na, Cu, Zn) remain essentially

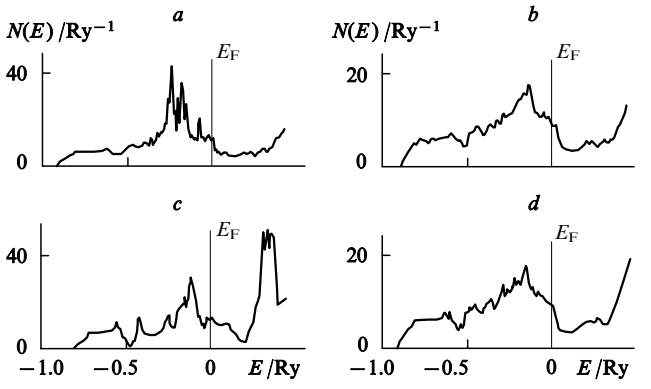


Figure 12. Total densities of states for $Mg_{0.75}Cu_{0.25}B_2$ (*a*), $Mg_{0.72}Na_{0.75}B_2$ (*b*), CaB_2 (*c*) and MgB_2 (*d*).[124]

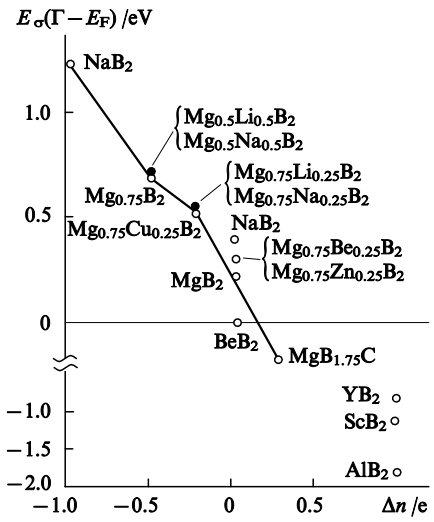


Figure 13. Dependence of the σ-band position at the Γ point of the Brillouin zone relative to the Fermi level in crystals $[E_\sigma(\Gamma - E_F)]$ on the electron concentration (relative to MgB_2, Δn) for binary diborides and ternary solid solutions based on MgB_2.[124]

similar to that of superconducting MgB_2 (see Fig. 12 and Table 4). The $N(E_F)$ value depends first of all on the impurity concentration. Hence, the main procedure for modifying the properties of magnesium diboride is to dope its cation sublattice. In addition to the VEC, electron distributions and superconductivity were also found to be dependent on the impurity concentration that affects structure peculiarities of MgB_2-based multicomponent solid solutions (first of all, the ratio between the in-plane distance and interlayer spacing).

Calculations of solid solution $Mg_{0.5}Al_{0.5}B$ [125] revealed the presence of hole states near the Z point of the Brillouin zone. It was also found that cation substitution and corresponding electron distributions cannot be completely described using the rigid band model.

Changes in the energy band structure with concentration and, in particular, the dependence of the σ-band energies on the composition of solid solutions $Mg_{1-x}Al_xB_2$ and $Mg_{1-x}Na_xB_2$ (x = 0, 1/3, 2/3, 1.0) were studied[126] using the density functional theory in the framework of supercell approach ($\sqrt{3} \times \sqrt{3}$) (Fig. 14). For $Mg_{1-x}Na_xB_2$ with any x, the top of the B p_{xy}-band at the Γ point is above E_F; in other words, the major electronic criterion for the existence of superconductivity holds. For $Mg_{1-x}Al_xB_2$, this condition is valid at $x < 0.6$. At $x > 0.6$, the hole states at the centre of the Brillouin zone disappear. The concentrations of the σ-holes (n_h /cm^{-3}) depend on the compositions of solid solutions as follows:[126]

for $Mg_{1-x}Al_xB_2$, $n_h = (0.8 + 0.8x) \times 10^{23}$,

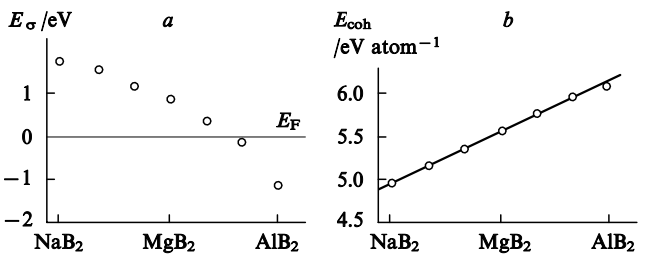


Figure 14. Changes in the σ-band position at the Γ point of the Brillouin zone (E_σ) relative to the Fermi level (*a*) and cohesive energies (*b*) in the order $NaB_2 \rightarrow Mg_{1-x}Na_xB_2 \rightarrow MgB_2 \rightarrow Mg_{1-x}Na_xB_2 \rightarrow AlB_2$.[126]

for $Mg_{1-x}Na_xB_2$, $n_h = (0.8 - 1.4x) \times 10^{23}$.

The hole concentration is a maximum ($\sim 1.6 \times 10^{22}$ cm^{-3}) for NaB_2. The cohesive energy (see Fig. 14) monotonically increases in the order $NaB_2 < Mg_{1-x}Na_xB_2 < MgB_2 < Mg_{1-x}Al_xB_2 < AlB_2$ as the corresponding bonding states in the valence band are filled.

b. Experimental studies

Theoretical studies of systems mentioned above are accompanied by experimental search [83, 136, 153–159] for new superconductors based on MgB_2 (variation of its elemental composition was mostly considered). Substitution solid solutions were synthesised using cation ($Mg_{1-x}M_xB_2$; M = Li, Be, Al, Zn, Cu) [83, 136, 153–155] and anion ($MgB_{2-y}C_y$) [156–158] sublattice substitution. Earlier,[159] only the formation of solid solutions in the MgB_2–AlB_2 system was reported.

Solid solutions were synthesised from elements in inert atmosphere, the samples obtained were analysed by elemental and structural analyses and their superconductivity parameters (T_c, ΔT_c) were measured (Table 5).

System Mg–B–Be.[155] A mixture of MgB_2 + BeB_2 phases was obtained. Beryllium diboride has a hexagonal structure (the space group $P6/mmm$, $c/a = 0.977$) and is paramagnetic at $T < 5$ K. It was found that beryllium does not replace the Mg atoms.

System Mg–B–Li.[155] The homogeneity region of solid solutions $Mg_{1-x}Li_xB_2$ was determined ($x < 0.3$). As lithium content increases, the interlayer distance remains unchanged while the in-plane B–B distance (parameter a) is shortened by ~0.014 Å (at $x = 0.3$). A decrease in T_c is observed beginning with $x = 0.1$ and becomes pronounced near the single-phase composition bound of the solid solution ($x = 0.3$). Loss of superconductivity occurs for the sample with $x = 0.5$.

System Mg–B–Al.[83] Two homogeneity regions of solid solutions $Mg_{1-x}Al_xB_2$ were found (see Table 5). As the Al/Mg ratio increases, anisotropic lattice compression occurs: the interlayer spacings decrease appreciably while the B–B distances do not exhibit considerable changes. This leads to structural instability of the crystal and phase transition at $x = 0.1$. A decrease in T_c in the homogeneity region of the solid solutions was explained [83] by an increase in the electron concentration and a decrease in $N(E_F)$. Analysis of the phase diagram shows that the superconducting phase is very close to the structural instability point of the system.

System Mg–B–Cu.[153, 154] Information about this system is contradictory. Abnormally high T_c = 49 K announced [153] for a sample with stoichiometric composition $Mg_{0.8}Cu_{0.2}B_2$ has not been confirmed; attempts at preparing copper-containing single-phase solid solutions failed.[154]

System Mg–B–Zn.[154] The homogeneity region for $Mg_{1-x}Zn_xB_2$ samples is up to $x = 0.1$. Analysis of the lattice parameters for a sample with $x = 0.1$ revealed their increase compared to those of MgB_2, namely, 0.17% for a and 0.2% for c. It was suggested [154] that nonmonotonic change in T_c is due to positive for the parameter a (in-plane B–B distances) and negative for the parameter c (interlayer spacings) expansion effects.

System Mg–B–C.[156–158] AlB_2-Type borocarbides $MgB_{2-x}C_x$ were synthesised from elements. Transition temperature T_c decreases in the homogeneity region ($x \leqslant 0.20$) by ~2 K (at $x = 0.20$, see Ref. 157) while the width of the transition, ΔT_c, substantially increases (by ~3–7 K as compared to 'pure' MgB_2, see Refs 156, 157). Introduction of carbon impurity leads to compression of graphite-like boron sheets: $a(MgB_2) - a(MgB_{1.8}C_{0.2}) = 0.013$ Å. The interlayer distances (the lattice parameter c) remain unchanged.[156] Magnesium borocarbides with much narrower homogeneity region ($x < 0.1$) were also synthesised;[158] transition temperature of these compounds decreases as the C/B ratio increases.

Table 5. Conditions for synthesis and characteristics of particular ternary systems based on MgB_2.

Starting materials [a]	Reaction conditions	Products (phase composition)	T_c /K	Lattice parameters /Å		Ref.
				a	*c*	
Mg + B + Al	95% Ar + 5% H_2, 600–900 °C	$Mg_{1-x}Al_xB_2$: solid solutions at $0 < x < 0.1$ and $0.25 < x < 0.40$ mixture of phases at $0.1 < x < 0.25$	38 ($x = 0$) 36 ($x \approx 0.1$) 0 ($x > 0.1$)	decreases as x increases		83
Mg + B + Cu	95% Ar + 5% H_2, 600–900 °C	$Mg_{0.8}Cu_{0.2}B_2$ (?) [mixture of phases $MgB_2 + Cu_2Mg + MgO$ (traces)]	49 (?)	3.068	3.505	153
	100% Ar, 600–900 °C	mixture of phases $MgB_2 + Cu_2Mg +$ + (MgO + MgB_4) (traces)	(?)	–	–	154
Mg + B + Zn	100% Ar 600–900 °C	solid solutions $Mg_{1-x}Zn_xB_2 + MgO$ (traces) + MgB_4 at $x \approx 0.1$, mixture of phases at $x > 0.1$	changes nonmonotonically	3.0841 ($x \leqslant 0.1$)	3.5250 ($x = 0.1$)	154
Mg + B + Li	100% Ar, 950 °C	$Mg_{1-x}Li_xB_2$: solid solutions at $x < 0.3$ mixture of phases at $x > 0.3$	decreases as x increases	3.070 ($x = 0.3$)	3.524 ($x = 0.3$)	155
Mg + B + Be	Ar	mixture of phases	–	–	–	136
Mg + B + C	100% Ar, 850 °C, 20 atm	$MgB_{1.8}C_{0.2}$ + MgO (traces)	$T_{c1} \approx 41$ $T_{c2} \approx 37$	3.070	3.520	156
	950 K	the same	~34	3.070	3.523	157

[a] Amorphous boron powder was used in most cases.

The synthesis of 'superstoichiometric' compositions $Mg_{1+x}B_2$ with 10 at.%, 20 at.% and 30 at.% of excess Mg added to the reaction mixture has also been reported.[157] It was found that 'superstoichiometry' has no effect on the superconductivity in magnesium diboride.

4. Materials science and some aspects of practical utilisation of MgB_2

a. Pressure dependence

Studies on the effect of pressure (as well as joint effect of pressure and temperature) on the properties of MgB_2 attract considerable attention both in solving fundamental problems of the nature of superconductivity in anisotropic media and in developing new procedures for improving the properties of superconducting MgB_2.[120, 160–166]

The structure of MgB_2 polycrystals as function of hydrostatic pressure up to 0.62 GPa was studied by neutron diffraction in the temperature range from 11 to 297 K.[163] It was found that the lattice parameters a and c change linearly with pressure, *viz*., $a = a_0 - 0.00187P$, $c = c_0 - 0.00307P$, where a_0 and c_0 are the lattice parameters under normal conditions and P is the pressure (in GPa). Essentially nonuniform lattice compression was emphasised: compression along the c axis is 64% larger than along the a axis (in the B–B plane). Similar results were obtained in synchrotron X-ray diffraction studies of isothermal compression (Fig. 15). Thermal expansion of the crystal lattice is also anisotropic and is mainly due to changes in the interlayer distances (the parameter c).[163] It was found that the effect is due to anisotropy of chemical bonding in MgB_2.[120–163]

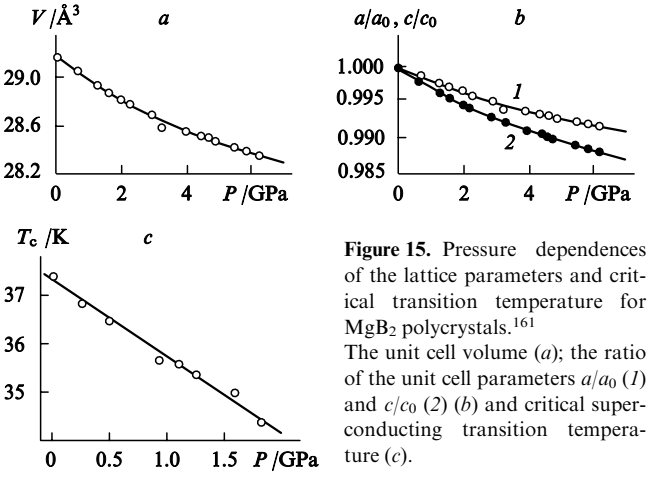


Figure 15. Pressure dependences of the lattice parameters and critical transition temperature for MgB_2 polycrystals.[161]
The unit cell volume (*a*); the ratio of the unit cell parameters a/a_0 (*1*) and c/c_0 (*2*) (*b*) and critical superconducting transition temperature (*c*).

Superconductivity parameters of MgB_2 are pressure dependent. For instance, it was found that the superconducting transition temperature decreases with a rate of -2.0 [162] and -1.6 K $(GPa)^{-1}$,[164] respectively (see Fig. 15). This is consistent with the results of calculations [165] [-1.4 K $(GPa)^{-1}$] and can be explained based on the BCS theory of the mechanism of superconductivity in magnesium diboride.[120, 165]

b. Neutron irradiation

Experiments [167] on thermal ($\Phi = 1 \times 10^{19}$ cm^{-2}) and fast ($\Phi = 1 \times 10^{18}$ cm^{-2}) neutron irradiation of MgB_2 (the total dose was greater than 10 doses per atom) were carried out with a IVV-2M nuclear reactor at $T = 350$ K. The transition temperature of irradiated samples decreased from 40 to 5 K, the residual resistance ρ_0 increased (from 0.35 to 2.0 mΩ cm) and the upper critical field exhibited minor changes ($-dH_{c2}/dT \approx 0.5$ T K^{-1}). By analogy with A15-type superconductors (Nb_3Sn, V_3Si), the results obtained were explained [167] by a decrease in $N(E_F)$. It was concluded that high radiation resistance of MgB_2 under conditions of neutron irradiation (other superconductors undergo amorphisation under such conditions) is of prime importance for practical utilisation of this compound. Irradiation of MgB_2 samples leads to anisotropic lattice expansion (mostly, to an increase in the parameter c from 3.5216 to 3.5533 Å), which is accompanied by an increase in the unit cell volume by ~1.4%.[157] The occupation number of Mg sites decreases from 0.94 to 0.89, while the occupation number of B sites remains unchanged. No antisite defects were found.

c. Grain boundary effects

Heat treatment of MgB_2 under high pressure to improve superconducting properties of highly porous (under the synthesis conditions) magnesium diboride polycrystals has been proposed.[160] At $T = 950$ °C and $P = 3$ GPa, the surface morphology of MgB_2 samples changed, their porosity decreased and the grain boundary contact area increased. High-resolution transmission electron microscopy studies of the morphology of the MgB_2 samples obtained by high-pressure sintering ($P = 3$ GPa) revealed the absence of porosity and strong connections between grains. The impurity phase (magnesium tetraboride) occurred in the form of small inclusions.[113] Specific features of some properties of

MgB_2 polycrystals, determined by the grain structure of the surface, have been discussed.[168, 169]

d. Surface and films

The development of methods for reproducible synthesis of epitaxial superconducting MgB_2 thin films for various electronic devices is one of the key problems of practical utilisation of this material. Here, the use of many conventional film growth procedures is complicated by the large differences in vapour pressure, adsorption coefficients and mobilities between boron and magnesium as well as due to a tendency of magnesium to undergo oxidation.

Currently, such films are synthesised using two, *ex situ* and *in situ*, approaches.[170–178] The former[174, 175] implies preliminary preparation of boron films which are then saturated with magnesium while the latter includes fabrication of MgB_2 films during the same run.

Currently, films with the highest current density and T_c (37–39 K) have been obtained by *ex situ* processes.[174, 175] The procedure included pulsed laser deposition (PLD) of thin boron films onto a substrate ($SrTiO_3$) followed by their reaction with magnesium vapours at 900 °C. The film surfaces were characterised[175] by well-developed grain structure. This approach has a drawback, that is, the high-temperature stage (here, temperatures are higher than the decomposition temperature of magnesium diboride). Therefore, this method is inapplicable to the growth of multilayers and heterojunctions. In addition, in the case of *ex situ* synthesis the film growth is driven by diffusion of magnesium through an already formed magnesium diboride surface layer, which makes it difficult to obtain an epitaxial relationship between the film and the substrate.[174, 175]

The *in situ* film growth involves two stages.[170–173] Initially, magnesium diboride films are prepared by PLD of various targets on different substrates, *e.g.*, Al_2O_3, $LaAlO_3$, $SrTiO_3$.[173] The targets (Fig. 16) were dispersed (< 45 μm) powders of MgB_2 synthesised from elemental boron and magnesium, commercial MgB_2 powders (AA), *etc*. Typically, the films were 100–500 nm thick. Superconductivity was observed only for films annealed in the rather narrow temperature interval (550–600 °C). Atomic force microscopy images revealed a reasonably smooth surface of these films, which is in stark contrast to the surface of the *ex situ* prepared films with well-defined grains. Films were deposited on the (100) and (111) surfaces of $SrTiO_3$ by (i) PLD of MgB_2, (ii) PLD of multilayers of MgB_2 and Mg followed by *in situ* annealing at high temperature and (iii) PLD of multilayers of Mg and B followed by *in situ* annealing at high temperature.[174] The highest superconducting transition temperature (T_c = 22 K) was observed for the films grown from magnesium diboride target. An increase in the annealing temperature deteriorates the superconductivity characteristics (for instance, T_c was no higher than 8 K after annealing at temperatures > 800 °C). This is thought to be due to layer-by-layer deviation from perfect nonstoichiometry.[174] It was emphasised that the necessary condition for growth of superconducting films consists in retaining the necessary Mg content.

Films grown *in situ* from room-temperature deposited Mg + MgB_2 powder targets and post-annealed at 600 °C were also characterised by relatively low T_c (12–22 K). It is believed that one of the key factors consists in the choice of reaction conditions to prevent oxidation of magnesium in plasma and in the film deposited. In this case, of great importance is the choice of the pressure of the inert gas in the vacuum chamber. Yet another reason for the low T_c is associated with the possibility[172] of formation of nonsuperconducting higher magnesium borides (MgB_4, MgB_7) and elemental boron, which deteriorates the superconductivity parameters of the film. The formation of magnesium borides is associated with the nature of plasma generated by the laser. In different ionisation zones, the temperature of plasma can be as high as several thousands of degrees. In this connection, of great importance are the results of thermodynamic modelling[179] of the system Mg–B using the CALPHAD technique.[180] Calculations[179] of composition–temperature, composition–pressure and pressure–temperature phase diagrams were carried out using experimental values of thermodynamic parameters of the components (MgB_2, MgB_4, MgB_7 as well as the gas, liquid and solid magnesium phases and β-boron). Magnesium diboride can be formed only at vapour pressures of magnesium falling into specific range and in particular temperature range (Fig. 17). Clearly, operation under these conditions will favour optimisation of the composition and, as a consequence, superconductivity characteristics of *in situ* grown films.

A 'mixed' film fabrication procedure has been proposed.[177] Films deposited *in situ* from MgB_2 targets in high vacuum exhibited the properties of pure metals or semiconductors; super-

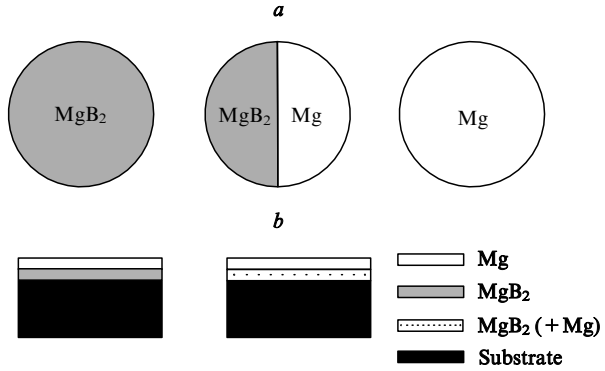


Figure 16. Schematical drawings of the targets (*a*) and chemical compositions of *in situ* prepared films (*b*).[173]

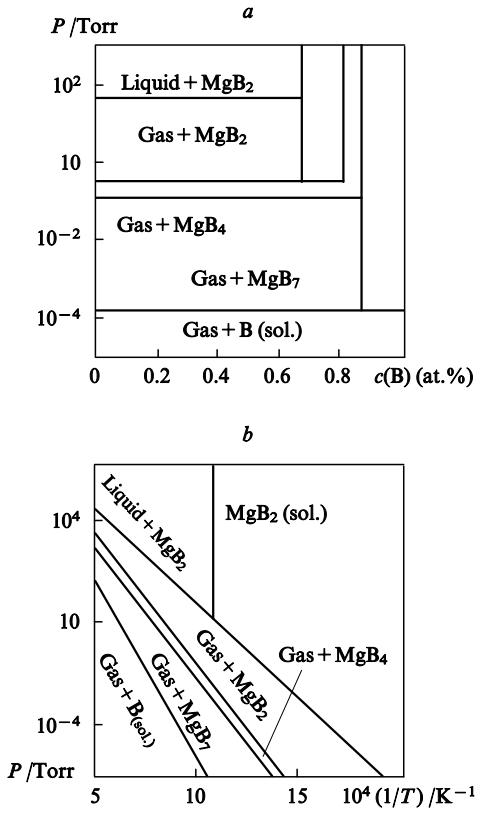


Figure 17. Calculated diagrams of the Mg–B system.
The pressure–composition diagram at T = 850 °C (*a*) and P–T-diagram for the ratio Mg : B > 1 : 2 (*b*). The 'gas + MgB_2' region corresponds to thermodynamic conditions for the preparation of MgB_2 thin films. Obtained from CALPHAD calculations.[179]

conductivity ($T_c \approx 25$ K) was observed only after additional exposure to magnesium vapours. Films with $T_c = 24$ K were obtained from stoichiometric MgB_2 targets by PLD on silicon substrates followed by heating in Ar atmosphere.[178] Uniform surface morphology and thickness of films were pointed out. Oxygen contamination of the outermost layers was assumed to be the main reason for the low T_c.

Vasquez *et al.*[181] reported a special XPS study of the elemental composition of the surface of MgB_2 polycrystals. The XPS spectrum of the surface of initial sample exhibited strong impurity signals from C and O, two signals from Mg 2*p*-state with binding energies (E_b) of 49.5 and 50.8 eV and signals from B 1*s*-states. Among the last-named group of signals, a weak peak with $E_b = 193$ eV is due to the presence of boric anhydride. The main signal of the B 1*s*-state was a doublet with the energies $E_b = 186.7$ and 187.9 eV comparable with the corresponding energies for isostructural *d*-metal diborides (187.2 – 188.5 eV, see Ref. 182).

According to Vasquez *et al.*[181] there are three main concentration zones near the MgB_2 surface. The first zone, *i.e.*, the surface of initial sample, is covered with oxide film and is substantially enriched with magnesium (the Mg : B ratio is 1 : 1.25). The oxide layer can be efficiently removed in the course of chemical purification (by, *e.g.*, 1% and 0.5% solutions of HCl and Br_2 in ethanol). The second, 'subsurface', zone under the oxide film is, on the contrary, depleted of magnesium (Mg : B = 1 : 3). In this zone, nonstoichiometry with respect to magnesium leads to a decrease in the electron density in boron sheets. The corresponding signal of B 1*s*-state is observed at higher binding energy ($E_b = 187.9$ eV). The second B 1*s*-peak ($E_b = 186.7$ eV) corresponds to the states of boron atoms in the third zone (magnesium diboride bulk with stoichiometric ratio Mg : B = 1 : 2). The energies of Mg 2*p*-level and Auger-signal are lower than that of metallic magnesium due to cationic state of Mg^{2+} in magnesium diboride.

e. New MgB_2-based superconducting materials: wires, ribbons, composites

A simple procedure for fabricating high density MgB_2 wires has been developed.[183] As mentioned above, MgB_2 polycrystals are obtained by solid-phase synthesis (a mixture of boron and magnesium powders is heat treated); mechanistically, magnesium diboride is formed *via* diffusion of Mg vapour into the boron grains. Bud'ko *et al.*[183] proposed to use this technique with boron fibres instead of powder. Boron fibres ($d \approx 100$ μm, Textron Systems, USA) and metallic magnesium taken in a stoichiometric ratio were placed in a Ta tube and heated at 950 °C for 1 h. Compared to the unreacted boron fibres, the MgB_2 wires thus obtained were brittle and somewhat deformed (see Fig. 18), but they did not break down. A tungsten core ($d \approx 15$ μm) of the starting boron fibres did not appear to be affected during the reaction, it also has no effect [183] on the superconducting characteristics of the MgB_2 wires. The diameter of the MgB_2 wires increased from 100 to 160 μm (synthesis of magnesium diboride powder is also accompanied by an increase in the particle size compared to the initial boron grains [82]). The density of wire segments was determined to be ~ 2.4 g cm^{-3} [$\sim 80\%$ of the theoretical density of MgB_2 crystal, 2.55 g cm^{-3} (see Ref. 82)]. The superconductivity parameters of the wires were $T_c = 39.4$ and $\Delta T_c = 0.9$ K. At room temperature, the wires exhibited the properties of highly conducting material (the resistivity, ρ, had a value of 9.6 μΩ cm), whereas near the critical transition temperature ($T = 40$ K) ρ decreased to 0.38 μΩ cm. Temperature dependence of the resistivity ($\rho = \rho_0 + \rho_1 T^{\alpha}$, where $\alpha \approx 2.6$) is close to that found for MgB_2 polycrystals [$\alpha \approx 2.8$, measured for $Mg(^{10}B)_2$ pellets].[82]

To choose optimum conditions for the preparation of superconducting MgB_2 wires, the mechanism of Mg diffusion into boron was systematically studied using commercialy sold boron fibres ($d = 100$ and 141 μm).[184] Boron fibres were exposed to magnesium vapours at 950 °C, the course of the reaction was monitored by the scanning electron microscopy (SEM) using the

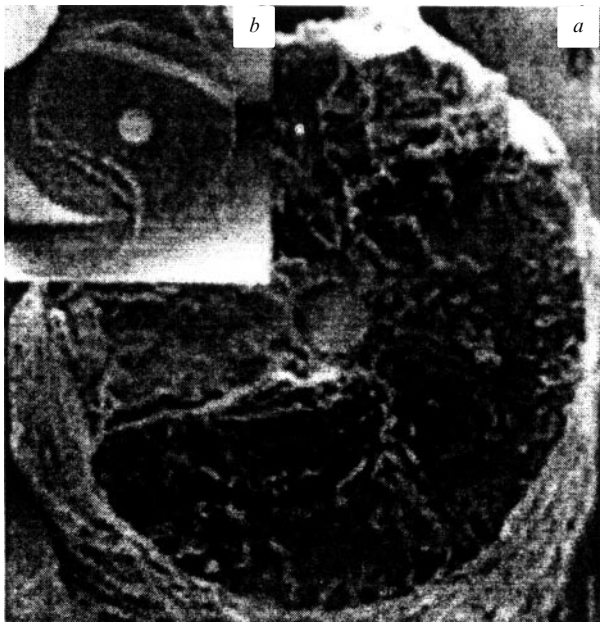


Figure 18. Electron microscope images of cross-section of a MgB_2 wire of diameter 160 μm (*a*) and unreacted boron filament with a tungsten core (*b*).[183]

SEM images of the cross-sections of the MgB_2 wires taken after time intervals. It was found that magnesium diboride begins to form after 15 min and is 50% complete after 1 h. The wire segments thus produced were of little porosity. In Fig. 19, the resistivities of MgB_2 pellets and wires are shown as functions of temperature. Different behaviour of the curves is thought to be due to larger density of wires.[184] Studies [185] on magnetotransport characteristics of dense wires revealed a very narrow resistive transition, a linear temperature dependence of H_{c2} in the range 7 K < T < 32 K and a positive curvature of this dependence near T_c. This is similar to the behaviour of layered IBC.[186–188]

Another technique for fabrication of superconducting MgB_2 wires involves placing powdered MgB_2 inside a sheath (a niobium,[189] gold, copper of nickel tube [190]). For instance, a niobium tube of diameter 6 mm was filled with MgB_2 powder and then a ribbon was prepared by cold drawing followed by rolling.[189] The ribbon with a superconducting core (a cross-section of 0.232 mm^2) had a cross-section of 2.56×0.32 mm^2.[189] At 4.2 K, the measured current density in the ribbons heated at 900 °C for 1, 2 and 3 h in an Ar atmosphere was 4.7, 7.5 and 1.1×10^4 A cm^{-2}, respectively. Experiments [190] with ribbons

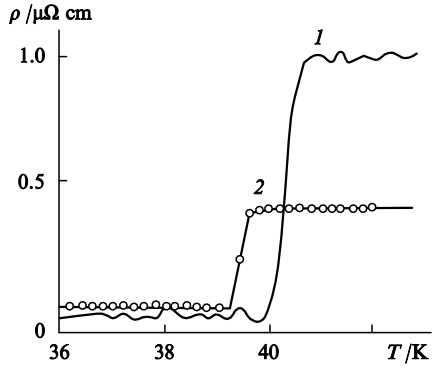


Figure 19. Resistivity of a dense MgB_2 wire (*1*) and polycrystalline MgB_2 pellet (*2*) as function of temperature.[184]

sheathed with different metals (Au, Ni, Cu) revealed the highest current density ($\sim 10^5$ A cm^{-2}) at 4.2 K for the ribbon with Ni sheath.

Magnesium diboride is highly brittle, which is typical of ceramics. Therefore, the problem of improving mechanical properties of MgB_2, *i.e.*, making the material more malleable without significant deterioration of its superconducting properties is of great importance. The most obvious way is to fabricate composites with ductile metals (or alloys) which should have low melting temperatures comparable with that of MgB_2 (1073 K) and be conductors and highly plastic substances. The formation of such composites should also not be accompanied by reactions between the ductile additive and magnesium diboride resulting in solid solutions. Recently, aluminium (T_m = 933 K) was found to be appropriate for this purpose.[191] Pellets of MgB_2–Al composite (11 vol.% Al) were prepared from MgB_2 (AA) and Al powders (the particle size of both components was 1 to 3 μm) by pressing at 500–700 K, *i.e.*, below the formation temperature of nonsuperconducting $Mg_{1-x}Al_xB_2$ solid solutions.[83] The samples were studied by scanning tunnelling microscopy and the transport and magnetic characteristics of the composites were measured. Particular attention was given to the proximity effect (the formation of a typical 'mini-gap' structure was observed, which is due to contact between magnesium diboride and aluminium, T_c^{Al} = 1.2 K) and to the effect of structural disordering on the superconducting transition temperature of the MgB_2–Al composite. The T_c value for the composite (38 K) was found to be comparable with that of pure MgB_2 (39 K).

IV. Conclusion

Information collected and systematised in this review describes the infancy of research into the properties of recently found new superconductor, MgB_2. In spite of short time that elapsed after the discovery of superconductivity in MgB_2, experimentalists and theoreticians have accumulated a great body of information about its physicochemical properties. The results obtained are of crucial importance for an understanding of the nature of superconductivity in anisotropic media. They gave a strong impetus to search for new superconductors among metal borides and related compounds and opened attractive prospects for their technological utilisation.

The state-of-the-art in this field can be outlined as follows. To date, a number of methods for the synthesis of MgB_2 have been developed. Peculiarities of the electronic structure and chemical bonding in MgB_2 as well as its electrophysical, magnetic, thermodynamic properties and spectroscopic characteristics have been studied. Based on the results of theoretical modelling and synthetic experiments, some new MgB_2-based solid solutions have been found and ways to further search for new superconductors have been directed. Materials science studies allowed the obtaining of MgB_2 powders, films, wires and composites.

On the other hand, magnesium diboride, as a medium-T_c superconductor, remains a unique compound in its kind except for a few solid solutions based on this substance. All attempts at increasing the critical transition temperature of MgB_2 or finding new superconductors with close T_c have failed so far. Many problems of the synthesis and detailed investigations of multicomponent systems with participation of magnesium diboride are still to be solved. These are, *e.g.*, studies of the phase diagrams, determination of homogeneity regions of solid solutions and criteria for optimum doping of MgB_2 as well as establishment of reasons for changes in T_c. Further search for new candidates for superconductors with graphite-like boron sheets in their structure is undoubtedly required. We believe that these problems will be the focus of research interest in the near future.

* * *

Studies on superconducting MgB_2 and related compounds have been continued in the course of preparation of the manuscript. The most interesting recent results are as follows.

Single crystals of MgB_2 have been first obtained.[192–195] A magnesium-enriched precursor sealed in a niobium ampoule was placed in a quartz tube,[192] heated to 1050 °C (1 h) and then very slowly cooled down to 700 °C (the cooling duration was 120 to 360 h). The MgB_2 single crystals were found to have various shapes (spherical, rod-like, or hexagonal-plate) depending on the cooling regime. The samples studied were characterised by excellent superconductivity parameters (T_c = 38 K and ΔT_c = 0.3 K). Experiments with MgB_2 single crystals revealed strong anisotropy of superconductivity.[192–195]

An original method for the synthesis of high density, single-phase MgB_2 ceramics with T_c = 38 K by crystallisation of magnesium diboride melt under pressure has been proposed.[196] The slope and the onset of transition to the superconducting state were found to be dependent on the grain size of the material.

Epitaxially grown, oriented MgB_2 films were prepared and their properties have been studied:[197–210] superconductivity,[197, 199–210] the Hall effect [207] and surface resistance.[206] Anisotropy of some characteristics of the oriented films (in particular, conductivity and upper critical field [198, 200]) was revealed. Degradation of superconductivity in MgB_2 films in the presence of water has been studied.[205] Preparation of nanostructured superconducting MgB_2 films has also been reported.[203] Pioneering calculations of the electronic structure of the boron- and magnesium-terminated MgB_2 (0001) surfaces have been carried out.[211, 212]

Summing up, mention may be made that there are three main lines of inverstigations in the field of search for MgB_2-related superconductors. The first research avenue is associated with extension of the class of possible MgB_2-based superconductors by varying their chemical compositions to obtain different types of solid solutions or by forming superstructures (see Section III.3). The second investigation line includes studies of a much broader spectrum of substances. Here, the search for possible superconductors has been performed among binary or multicomponent compounds which are to some extent structurally or chemically similar to MgB_2. The discovery of critical transitions in ZrB_2 (5.5 K, see Ref. 213), TaB_2 (9.5 K, see Ref. 137), Re_3B (4.7 K, see Ref. 214) and in the new phase of beryllium boride with the chemical composition $BeB_{2.75}$ and the unit cell containing 110.5 atoms (0.72 K, see Ref. 215) represent recent advances in this field.

The third line of research activity was initiated by the discovery of superconductivity at $T_c \approx 8$ K in a perovskite-like intermetallide $MgCNi_3$.[216] From the standpoint of 'renewed chemical paradigm' it was proposed [216] that the whole class of intermetallides should be considered as potential superconductors. The results obtained by Cava *et al.*[216] are of particular interest for the following reasons.

Highly symmetric structure of $MgCNi_3$ (the space group $Pm3m$) favours superconductivity. However, superconductivity in all the known isostructural compounds — oxide perovskites [*e.g.*, (Ba, K)BiO_3, see Ref. 217] — is due to electron–hole states of the oxygen atoms occupying 3*c*-type positions (0, 1/2, 1/2). Since in the $MgCNi_3$ structure these positions are occupied by Ni atoms, the mechanism of superconductivity should be of fundamentally different nature.

Most of the known 'non-oxide,' perovskite-like compounds MXM'_3 (M′ = Zn, Al, Ga, In, Sn; M = Mn, Fe; X = C, N) are ferromagnetic (and antiferromagnetic) or are characterised by more complex (mixed) types of spin ordering.[218] Hence, among structurally similar compounds, $MgCNi_3$ can be considered as an 'intermediate' between the classes of perovskite-like superconductors (oxides) and magnetics (non-oxide perovskites).

Among superconductors, nickel-containing IBC $LuNi_2B_2C$ ($T_c \approx 16$ K) and YNi_2B_2C ($T_c \approx 15.6$ K) are the closest 'chemical analogues' of $MgCNi_3$. However, unlike the last-named compound, these IBC belong to magnetic superconductors and exhibit

a distinct quasi-2D structure.[22] In addition, the Ni content in IBC is much less than in $MgCNi_3$. Taking into account clearly defined magnetic properties of nickel, the fact that superconductivity occurs in the nickel-rich compound $MgCNi_3$ is quite surprising.

Based on the results of pioneering studies on the properties of $MgCNi_3$ (the critical field, H_{c2}, the Hall coefficient, *etc*.,[219–221]) and critical transition temperatures of $MgCNi_{3-x}M_x$ (M = Mn, Co, Cu) samples doped at Ni sites, the parent compound, $MgCNi_3$, was placed into the class of 'conventional' superconductors with electron–phonon interactions.[222,223] Band structure calculations for $MgCNi_3$ (see Refs 224–227) revealed a distinctive feature, *viz*., the presence of an intense DOS peak near the Fermi level. It was found that the major contribution to $N(E_F)$ comes from the Ni 3*d*-states (~88.2%). Band structure calculations for new $MgCNi_3$-like superconductors have been carried out. The possibility of superconductivity in a nonstoichiometric (with respect to C sublattice) perovskite, in perovskite-like $ScBNi_3$ and $InBNi_3$ as well as in $MgCCo_3$ and $MgCCu_3$ (all of them are isoelectronic and isostructural to $MgCNi_3$) has been discussed.[228]

The discovery of superconductivity in intermetallic compounds MgB_2 and $MgCNi_3$ with simple and highly symmetric structures has given a creative urge to search for application areas of these promising superconductors.

The author expresses his gratitude to N I Medvedeva, V G Zubkov, V N Diev and V G Bamburov for valuable discussions.

References

1. *Perspectivnye Tekhnol*. **8** (1–2) 1 (2001)
2. J Nagamatsu, N Nakagawa, T Muranaka, Y Zenitani, J Akimitsu *Nature (London)* **410** 63 (2001)
3. G V Samsonov, L Ya Markovskii, A F Zhigach, M G Valyashko *Bor, ego Soedineniya i Splavy* (Boron, Its Compounds and Alloys) (Kiev: Academy of Sciences of Ukr. SSR, 1960)
4. B Post, F W Glaser *Refractory Binary Borides* (New York: Interscience, 1963)
5. V Aronsson, T Lundstrom, S Rundquvist *Refractory Borides, Silicides and Phosphides* (London: Methuen, 1965)
6. E L Muettertis (Ed.) *The Chemistry of Boron and its Compounds* (New York: Wiley, 1967)
7. H Goldschmidt *Interstitial Alloys* (London: Butterworths, 1967)
8. G V Samsonov, T I Serebryakova, V A Neronov *Boridy* (Borides) (Moscow: Atomizdat, 1975)
9. G V Samsonov, I M Vinitskii *Tugoplavkie Soedineniya. Spravochnik* (High-Melting Compounds. Handbook) (Moscow: Metallurgiya, 1976)
10. Yu B Kuz'ma *Kristallokhimiya Boridov* (Crystal Chemistry of Borides) (L'vov: Vishcha Shkola, 1983)
11. T Ya Kosolapov (Ed.) *Boridy i Materialy na Ikh Osnove* (Borides and Materials Based on Them) (Kiev: Institute of Problem of Materials Technology, Academy of Sciences, Ukr. SSR, 1986)
12. Yu B Kuz'ma, I F Chaban *Dvoinye i Troinye Sistemy, Soderzhashchie Bor* (Binary and Ternary Systems Containing Boron) (Moscow: Metallurgiya, 1990)
13. T I Serebryakova, V A Neronov, P D Peshev *Vysokotemperaturnye Boridy* (High-Temperature Borides) (Moscow: Metallurgiya, 1991)
14. A L Ivanovskii, G P Shveikin *Kvantovaya Khimiya v Materialovedenii. Bor, ego Splavy i Soedineniya* (Quantum Chemistry in Materials Technology. Boron, Its Alloys and Compounds) (Ekaterinburg: Izd. Ekaterinburg, 1997)
15. S V Vonsovsky, Y A Izumov, E Z Kurmaev *Superconductivity of Transition Metals, Alloys and Compounds* (Berlin: Springer, 1982)
16. L E Toth *Transition Metal Carbides and Nitrides* (New York; London: Academic Press, 1971)
17. L Leyarovska, E Leyarovski *J. Less-Common Met*. **67** 249 (1979)
18. M B Maple, O Fischer (Eds) *Superconductivity in Ternary Compounds; I. Structural, Electronic and Lattice Properties; II. Superconductivity and Magnetism* (Berlin; Heidelberg; New York: Springer, 1982)
19. R J Cava, H Takagi, B Batlogg, H W Zandbergen, J J Krajewski, W F Peck, R van Doren, R J Felder, T Siegrist, T K Mizuhashi, J O Lee, H Eisaki, S A Carter, S Uchida *Nature (London)* **367** 146 (1994)
20. R J Cava, H Takagi, H W Zandbergen, J J Krajewski, W E Peck, T Siegrist, B Batlogg, R van Doren, R J Felder, T K Mizuhashi, J O Lee, H Eisaki, S Uchida *Nature (London)* **367** 252 (1994)
21. R Nakarajan, C Mazumdar, Z Nossian, S K Dhar, K V Gopalakrishnan, L C Gupta, C Goddart, B D Padalia, R Vijayaraghavan *Phys. Rev. Lett*. **72** 274 (1994)
22. A L Ivanovskii *Usp. Khim*. **67** 403 (1998) [*Russ. Chem. Rev*. **67** 357 (1998)]
23. H Moissan *Ann. Chim. Phys*. **6** 296 (1895)
24. A Stock *Hydrides of Boron and Silicon* (Ithaca, NY: Cornell University Press, 1933)
25. N Moissan *Ann. Chim. (Paris)* **8** 87 (1906)
26. F Jones, R Taylor *J. Chem. Soc*. 1881 (1912)
27. R Ray *J. Chem. Soc*. **105** 2162 (1914)
28. M Travers, N Gupta, R Ray *Indian Inst. Sci*. **1** 1 (1914)
29. M Travers, R Ray *Proc. R. Soc. London A* **87** 153 (1913)
30. T Serebryakova *J. Less-Common Met*. **67** 499 (1979)
31. P Duhart *Ann. Chim. (Paris)* **7** 339 (1962)
32. F A Shunk *Constitution of Binary Alloys (Second Suppl)* (New York: McGraw-Hill, 1971)
33. T Massalsky (Ed.) *Binary Alloy Phase Diagrams* (New York: A S M International, 1990)
34. M Jones, R Marsh *J. Am. Chem. Soc*. **76** 1434 (1954)
35. V Russel, R Hirst, F Kanda, A J King *Acta Crystallogr*. **6** 870 (1953)
36. L Ya Markovskii, Yu D Kondrashev, G V Kapustovskaya *Zh. Obsh. Khim*. **25** 433 (1955) [a]
37. L Ya Markovskii, Yu D Kondrashev, G V Kapustovskaya *Dokl. Akad. Nauk SSSR* **100** 1095 (1955) [b]
38. P Beck (Ed.) *Electronic Structure and Alloy Chemistry of the Transition Elements* (New York; London: Wiley-Interscience, 1963)
39. K Schubert *Kristallstrukturen zweikomponentiger Phasen* (Berlin; Gottingen; Heidelberg: Springer, 1964)
40. W B Pearson *The Crystal Chemistry and Physics of Metals and Alloys* (New York; London; Sidney; Toronto: Wiley-Interscience, 1972)
41. A Guette, R Naslain, J Galy *C.R. Acad. Sci., Ser. C* **275** 41 (1972)
42. R Naslain, A Guette, M Barret *J. Solid State Chem*. **8** 68 (1973)
43. R Naslen, A Guette, J Casper, in *Bor. Poluchenie, Struktura, Svoistva* (Boron. Production, Structure, Properties) (Moscow: Nauka, 1974) p. 160
44. R Naslain, A Quette, P Hagenmuller *J. Less-Common Met*. **47** 1 (1976)
45. A Quette, M Barret, R Naslain, P Hagenmuller *J. Less-Common Met*. **82** 325 (1981)
46. I I Tupitsyn, I I Lyackovskaya, M S Nakhmanson, A A Sukhik *Sov. Phys.-Solid State* **16** 2915 (1975)
47. D Armstrong, P G Perkins *J. Chem. Soc., Faraday Trans. 2,* **75** 12 (1979)
48. J K Burdett, G J Miller *Chem. Mater*. **2** 12 (1989)
49. A L Ivanovskii, N I Medvedeva *Zh. Neorg. Khim*. **45** 1355 (2000) [c]
50. G P Shveikin, A L Ivanovskii *Usp. Khim*. **63** 751 (1994) [*Russ. Chem. Rev*. **63** 711 (1994)]
51. A F Guillermet, G Grimvall *J. Less-Common Met*. **169** 257 (1991)
52. X Wang, D Tian, L Wang *J. Phys., Condens. Matter* **6** 10185 (1994)
53. A L Ivanovskii, N I Medvedeva, Yu E Medvedeva *Mendeleev Commun*. 129 (1998)
54. A L Ivanovskii, N I Medvedeva, Yu E Medvedeva, A E Nikiforov, G P Shveikin *Metallofiz. Noveishie Tekhnol*. **20** 41 (1998)
55. A L Ivanovskii, N I Medvedeva, Yu E Medvedeva *Metallofiz. Noveishie Tekhnol*. **21** 19 (1999)
56. A L Ivanovskii, N I Medvedeva, Yu E Medvedeva, G P Shveikin *Dokl. Akad. Nauk* **361** 642 (1998) [b]
57. A L Ivanovskii, N I Medvedeva *Zh. Neorg. Khim*. **44** 1717 (1999) [c]
58. S Nakano, O Fukunaga *Diam. Relat. Mater*. **2** 1409 (1993)
59. G Bocquillon, C Loriers-Susse, J Lorieres *J. Mater. Sci*. **28** 3547 (1993)
60. T Endo, O Fukunaga, M Iwata *J. Mater. Sci*. **14** 1676 (1979)
61. T I Serebryakova, V A Ponomarenko, A I Karasev *Poroshk. Metall*. (11) 77 (1980)

62. V B Shipilo, L M Gameza, I P Guseva *Sverkhtv. Mater.* (3) 5 (1981)
63. V B Shipilo, V V Sergeev *Poroshk. Metall.* (4) 48 (1985)
64. V B Shipilo, L M Gameza *Zh. Fiz. Khim.* **63** 196 (1989) [d]
65. V B Shipilo, L M Gameza *Neorg. Mater.* **25** 51 (1989) [e]
66. V S Lysanov (Ed.) *El'bor v Mashinostroenii* (Elboron in Machine Building) (Leningrad: Mashinostroenie, 1978)
67. V L Solozhenko, V Z Turkevich, W B Holzapfel *J. Phys. Chem. B* **103** 8137 (1999)
68. T Ya Kosolapova, T V Andreeva, T V Bartnitskaya, G G Gnesin, G N Makarenko, I I Osipova, E V Prilutskii *Nemetallicheskie Tugoplavkie Soedineniya* (Nonmetallic High-Melting Compounds) (Moscow: Metallurgiya, 1985)
69. H Kobayashi, M Katoh, Y Kamiyama, T Mitamura *J. Ceram. Soc. Jpn.* **100** 172 (1992)
70. V Sundaran, K V Logan, R F Speyer *J. Mater. Res.* **12** 2657 (1997)
71. E G Gillan, R B Kaner *Chem. Mater.* **8** 333 (1996)
72. Y Guindon, L Rao, E G Gillan, R B Kaner *J. Mater. Res.* **10** 353 (1995)
73. M Gu, Z Wu, Y Jin, M Kocak *J. Mater. Sci.* **35** 2499 (2000)
74. J A Wilson, J W Steeds, D Wilkes, C M Ward-Close *J. Mater. Sci.* **36** 67 (2001)
75. V G Bamburov, O V Sivtsova, V P Semyannikov, V A Kiselev *Ogneupory Tekhn. Keram.* (2) 2 (2000)
76. Jpn. P. 62 108 710; *Chem. Abstr.* **107** 63 688 (1987)
77. Jpn. P. 5 105 532 ; *Chem. Abstr.* **119** 78 476 (1993)
78. Jpn. P. 5170 514; *Chem. Abstr.* **119** 187 176 (1993)
79. Jpn. P. 9 080 821; *Chem. Abstr.* **127** 26 010 (1997)
80. Jpn. P. 0 101 936; *Chem. Abstr.* **101** 11 276 (1984)
81. Jpn. P. 0 298 676; *Chem. Abstr.* **110** 140 420 (1989)
82. S L Bud'ko, G Lapertot, C Petrovic, C E Cunningham, N Anderson, P C Canfield *Phys. Rev. Lett.* **86** 1877 (2001)
83. J S Slusky, N Rogado, K A Regan, M A Hayward, P Khalifah, T He, K Inumaru, S M Loureiro, M K Haas, H W Zandbergen, R J Cava *Nature (London)* **410** 343 (2001)
84. D C Larbalestier, L D Cooley, M O Rikel, A A Polyanskii, J Jiang, S Patanik, X Y Cai, D M Feldman, A Gurevich, A A Squitiere, M T Naus, C B Eom, E E Hellstrom, R J Cava, K A Regan, N Rogado, M A Hayward, T He, J S Slusky, P Khalifah, K Inumaru, M Haas *Nature (London)* **410** 186 (2001)
85. J Kortus, I I Mazin, K D Belashchenko, V P Antropov, L L Boyer *Phys. Rev. Lett.* **86** 4656 (2001)
86. K D Belashchenko, M van Schlifgaarde, V P Antropov http://xxx.lanl.gov/abs/cond-mat/0102290 (2001)
87. J M An, W E Pickett *Phys. Rev. Lett.* **86** 4366 (2001)
88. J Gavaler *Appl. Phys. Lett.* **23** 480 (1973)
89. R J Cava, B Batlogg *MRS Bull.* **14** 49 (1989)
90. K Holczer, O Klein, S Huang, R B Kaner, K Fu, R L Whetten, F Diederich *Science* **252** 1154 (1991)
91. S Yamanaka, H Kawaij, K Hothehama, M Ohashi *Adv. Mater.* **8** 771 (1996)
92. H Kawaij, K Hothehama, S Yamanaka *Chem. Mater.* **9** 2127 (1997)
93. S Yamanaka, K Hotehama, H Kawaij *Nature (London)* **392** 580 (1998)
94. M Kohmoto, I Chang, J Friedel http://xxx.lanl.gov/abs/cond-mat/0103352 (2001)
95. N B Brandt, S M Chudinov, Y G Ponomarev *Modern Problems in Condensed Matter Sciences* Vol. 20 (North-Holland: Amsterdam, 1988)
96. I T Belash, A D Bronnikov, O A Zharikov, A V Palnichenko *Synth. Met.* **36** 283 (1990)
97. J H Schon, C Kloc, B Batlogg *Nature (London)* **408** 549 (2000)
98. R Osborn, E A Goremychkin, A L Kolesnikov, D G Hinks *Phys. Rev. Lett.* **87** 7005 (2001)
99. A Gerashenko, K Mikhalev, S Verkhovskii, T D'yachkova, A Tyutyunnik, V Zubkov http://xxx.lanl.gov/abs/cond-mat/0102421 (2001)
100. A G Joshi, C G Pillai, P Raj, S K Malik *Solid State Commun.* **118** 445 (2001)
101. T J Sato, K Shibata, Y Takano http://xxx.lanl.gov/abs/cond-mat/0102486 (2001)
102. O F de Lima, R A Ribeiro, M Avila, C A Cardoso, A A Coelho *Phys. Rev. Lett.* **86** 5974 (2001)
103. Ch Walti, E Felder, C Degen, G Wigger, R Monnier, B Delley, H R Ott http://xxx.lanl.gov/abs/cond-mat/0102522 (2001)
104. S X Dou, X L Wang, J Horvat, D Milliken, E W Collings, M D Sumption http://xxx.lanl.gov/abs/cond-mat/0102320 (2001)
105. D D Lawrie, J P Franck *Physica C* **245** 159 (1995)
106. K O Cheon, I R Fischer, P C Canfield *Physica C* **312** 35 (1999)
107. D K Finnemore, J E Ostenson, S L Bud'ko, G Lapertot, P C Canfield *Phys. Rev. Lett.* **86** 2420 (2001)
108. Y Takano, H Takeya, H Fujii, H Kumakura, T Hatano, K Togano, H Kito, H Ichara http://xxx.lanl.gov/abs/cond-mat/0102167 (2001)
109. S Li, H H Wen, Z W Zhao, Y Ni, Z A Ren, G C Che, H Yang, Z Y Li, Z H Zhao http://xxx.lanl.gov/abs/cond-mat/0103032 (2001)
110. C U Jung, M S Park, W N Kang, M S Kim, S Y Lee, S I Lee *Physica C* **353** 162 (2001)
111. W N Kang, C U Jung, K Kim, M S Park, S Y Lee, H Kim, E M Choi, M S Kim, S J Lee http://xxx.lanl.gov/abs/cond-mat/0102313 (2001)
112. H Kotegawa, K Ishida, Y Kitaoka, T Muranaka, J Akimitsu http://xxx.lanl.gov/abs/cond-mat/0102334 (2001)
113. G Y Sung, S H Kim, J Kim, D C Yoo, J W Lee, C U Jung, M S Park, W N Kang, D Zhonglian, S I Lee http://xxx.lanl.gov/abs/cond-mat/0102498 (2001)
114. A Sharoni, I Felner, O Millo *Phys. Rev. B* **63** 220508 (2001)
115. G Karapetrov, M Iavorone, W K Kwok, G W Gabtree, D G Hinks *Phys. Rev. Lett.* **86** 4374 (2001)
116. H Schmidt, J F Zasadzinski, K E Gray, D G Hinks *Phys. Rev. B* **63** 22 504 (2001)
117. B Gorshunov, C A Kutscher, P Haas, M Dressel, F P Mena, A B Kuz'menko, D van der Marel, T Muranaka, J Akimitsu *Eur. Phys. J. B* **21** 159 (2001)
118. R K Kremer, B J Gibson, J S Ahn http://xxx.lanl.gov/abs/cond-mat/0102432 (2001)
119. Y Wang, T Plackowski, A Junod *Physica C* **355** 179 (2001)
120. T Vogt, G Schneider, J A Hriljac, G Yang, J S Abell *Phys. Rev. B* **63** 220 505 (2001)
121. J E Hirsch *Science* **292** 1521 (2001)
122. J E Hirsch *Physica C* **341** – **348** 213 (2000)
123. W L McMillan *Phys. Rev. Ser. 2* **167** 331 (1968)
124. N I Medvedeva, A L Ivanovskii, J E Medvedeva, A J Freeman *Phys. Rev. B* **64** 220 502 (2001)
125. G Satta, G Profeta, F Bernardini, A Contonenza, S Massidda http://xxx.lanl.gov/abs/cond-mat/0102358 (2001)
126. S Suzuki, S Higai, K Nakao *J. Phys. Soc. Jpn.* **70** 1206 (2001)
127. I R Shein, N I Medvedeva, A L Ivanovskii *Fiz. Tv. Tela* (2001) (in the press) [f]
128. N I Medvedeva, Yu E Medvedeva, A L Ivanovskii http://zhurnal ape relarn ru/articles/2001/008 pdf (2000)
129. N I Medvedeva, Yu E Medvedeva, A L Ivanovskii *Dokl. Akad. Nauk* **379** (1) (2001) [b]
130. A Reyes-Serrato, D Galvan http://xxx.lanl.gov/abs/cond-mat/0103477 (2001)
131. E Z Kurmaev, I I Lyackovskaya, J Kortus, N Miyata, M Demeter, M Neumann, M Yanagihara, M Watanabe, T Muranaka, J Akimitsu http://xxx.lanl.gov/abs/cond-mat/0103487 (2001)
132. T A Callot, L Lin, G T Woods, G P Zhang, J R Thompson, M Paranthaman, D L Erderer http://xxx.lanl.gov/abs/cond-mat/0103593 (2001)
133. T Takahashi, T Sato, S Souma, T Muranaka, J Akimitsu *Phys. Rev. Lett.* **86** 4915 (2001)
134. N I Medvedeva, A L Ivanovskii, J E Medvedeva, A J Freeman, D L Novikov http://xxx.lanl.gov/abs/cond-mat/0104346 (2001)
135. C Beyreuther, R Hierl, G Wiech *Ber. Bunsenges. Phys. Chem.* **79** 1081 (1975)
136. I Felner *Physica C* **353** 11 (2001)
137. D Koczorowski, A J Zalevski, O J Zogal, J Klamut http://xxx.lanl.gov/abs/cond-mat/0103571 (2001)
138. A L Ivanovskii *Usp. Khim.* **66** 511 (1997) [*Russ. Chem. Rev.* **66** 459 (1997)]
139. N Sudo, H Hashizume, C Carvalho *J. Appl. Crystallogr.* **24** 286 (1991)

140. S V Okatov, A L Ivanovskii, N I Medvedeva, J E Medvedeva *Phys. Status Solidi A* **225** R3 (2001)
141. H Ripplinger, K Schwarz, P Blaha *J. Solid State Chem.* **133** 51 (1997)
142. S Massidda, A Continenza, T M DePascale, R Monnier *Z. Phys. B, Condens. Matter* **102** 83 (1997)
143. A L Ivanovskii, S V Okatov *Mendeleev Commun.* **11** 8 (2001)
144. S Fahy, D R Hamann *Phys. Rev. B* **41** 7587 (1990)
145. K Kusakabe, Y Tateyama, T Oguchi, S Tsuneyumi *Rev. High Pressure Sci. Technol.* **7** 193 (1998)
146. S Massidda, A Baldereschi *Solid State Commun.* **66** 855 (1985)
147. A H Silver, T Kushida *J. Chem. Phys.* **38** 865 (1963)
148. K Schwarz, H Ripplinger, P Blaha *Z. Naturforsch., A Phys. Sci.* **51** 527 (1996)
149. Y Kong, O V Dolgov, O Jepsen, O K Andersen *Phys. Rev. B* **64** 020501 (2001)
150. K Bohnen, R Heid, B Renker *Phys. Rev. Lett.* **86** 5771 (2001)
151. A Lin, I I Mazin, J Kortus http://xxx.lanl.gov/abs/cond-mat/0103570 (2001)
152. N I Mededeva, Yu E Medvedeva, A L Ivanovskii, V G Zubkov, A Friman *Pis'ma Zh. Eksp. Teor. Fiz.* **73** 378 (2001)
153. Y P Sun, W H Song, J M Dai, B Zhao, J J Du, H H Wen, Z X Zhao *Chin. Phys. Lett.* **18** 587 (2001)
154. S M Kazakov, M Angst, J Karpinski *Solid State Commun.* **119** 1 (2001)
155. Y G Zhao, X P Zhang, P T Qau, H T Zhang, S L Jia, B S Cao, M H Zhu, Z H Han, X L Wang, B L Gu http://xxx.lanl.gov/abs/cond-mat/0103077 (2001)
156. J S Ahn, E J Choi http://xxx.lanl.gov/abs/cond-mat/0103169 (2001)
157. S Zhang, J Zhang, T Zhao, C Rong, B Shen, Z Cheng *Chin. Phys.* **10** 335 (2001)
158. T Takenobu, T Ito, D H Chi, K Prassides, Y Iwasa http://xxx.lanl.gov/abs/cond-mat/0103241 (2001)
159. N V Vekshina, L Ya Markovskii, Yu D Kondrashev, T K Voevodskaya *Zh. Prikl. Khim.* **44** 958 (1971) [g]
160. C U Jung, M Park, W N Kang, K Kim, S Y Lee, S Lee *Physica C* **353** 162 (2001)
161. K Prassides, Y Iwasa, T Ito, D Chi, K Uehara, E Nushibori, M Takata, S Sakata, Y Ohishi, O Shimomura, T Muranaka, J Akimitsu *Phys. Rev. B* **64** 2509 (2001)
162. E Saito, T Taknenobu, T Ito, Y Iwasa, K Prassides, T Arima *J. Phys., Condens. Matter* **13** L267 (2001)
163. J D Jorgensen, D G Hinks, S Short *Phys. Rev. B* **63** 220508 (2001)
164. B Lorenz, R L Meng, C W Chu http://xxx.lanl.gov/abs/cond-mat/0102264 (2001)
165. I Loa, K Syassen *Solid State Commun.* **118** 279 (2001)
166. T Tomita, J J Hamlin, J S Schilling http://xxx.lanl.gov/abs/cond-mat/0103538 (2001)
167. A E Kar'kin, V V Voronin, T V D'yachkova, N I Kadyrova, A P Tyutyunnik, V G Zubkov, Yu G Zainulin, M V Sadovskii, B N Goshchitskii *JETP Lett.* **73** 570 (2001)
168. G Rubio-Bollinger, H Suderow, S Vieira *Phys. Rev. Lett.* **86** 5582 (2001)
169. A A Zhukov, K Yates, K G Perkins, Y Bugoslavsky, M Polichetti, A Berenov, J Driscoll, A D Caplin, L F Cohen *Supercond. Sci. Technol.* **14** L13 (2001)
170. W N Kang, H Kim, E Choi, C U Jung, S Lee http://xxx.lanl.gov/abs/cond-mat/0103179 (2001)
171. A Brikman, D Mijatovich, G Rijneders, V Leca, H Smodle, I Oomen, A A Golubov, F Roesthuis, S Hakema, H Hilgenkamp, D Blank, H Rogalla *Physica C* **353** 1 (2001)
172. D Blank, H Hilgenkamp, A Brikman, D Mijatovich, G Rijneders, H Rogalla *Appl. Phys. Lett.* **79** 394 (2001)
173. H M Christen, H Y Zhai, C Cantoni, M Paranthaman, B C Sales, R Rouleau, D P Norton, D K Christen, D Lowndes *Physica C* **353** 157 (2001)
174. S R Sinde, S B Ogale, R L Greene, T Venkatesan, P C Canfield, S L Bud'ko, G Lapertot, C Petrovic http://xxx.lanl.gov/abs/cond-mat/0103542 (2001)
175. C B Eom, M K Lee, J H Choi, L Belenky, X Song, L D Cooley, M T Naus, S Patanik, J Jiang, M Rickel, A Polyanskii, A Gurevich, X Y Cai, S D Bu, S E Babcock, E E Hellstrom, D C Larbalestier, N Rogano, K A Regon, M A Hayward, T He, J S Slusky, K Inumara, M K Haas, R J Cava *Nature (London)* **411** 558 (2001)
176. M Paranthaman, C Cantoni, H Y Zhai, H M Christen, T Aytug, S Sathyamuthy, E D Specht, J D Thompson, D H Lowndes, H R Kerchner, D K Christen *Appl. Phys. Lett.* **78** 3669 (2001)
177. G G Grassano, W Ramadan, V Ferrando, E Bellingeri, D Marre, C Ferdeghini, G Grasso, M Putti, A S Siri, P Manfrinetti, A Palenoza, A Chincarini http://xxx.lanl.gov/abs/cond-mat/0103572 (2001)
178. H Y Zhai, H M Chirsten, L Zhang, C Cantoni, M Paranthaman, B C Sales, D K Christen, D H Lowndes http://xxx.lanl.gov/abs/cond-mat/0103588 (2001)
179. Z K Liu, D G Schlom, Q Li, X Xi *Appl. Phys. Lett.* **78** 3678 (2001)
180. N Saunders, A P Miodownik *CALPHAD (Calculation of Phase Diagrams): a Comprehensive Guide* (Oxford: Pergamon Press, 1998)
181. R P Vasquez, C U Jung, M S Park, H-J Kim, J-Y Kim, S-I Lee *Phys. Rev. B* **64** 052510 (2001)
182. C L Perkins, R Singh, M Trenary, T Tanaka, Y Paderno *Surf. Sci.* **470** 215 (2001)
183. P C Canfield, D K Finnemore, S L Bud'ko, J E Ostenson, G Lapertot, C E Cunningham, C Petrovic *Phys. Rev. Lett.* **86** 2423 (2001)
184. S E Cunningham, C Petrovic, G Lapertot, S L Bud'ko, F Laabs, W Straszheim, D K Finnemore, P C Canfield *Physica C* **353** 5 (2001)
185. S L Bud'ko, C Petrovic, G Lapertot, C E Gunningham, P C Canfield *Phys. Rev. B* **63** 220503 (2001)
186. V Metlushko, U Welp, A Koshelev, I Aranson, G Crabtree, P C Canfield *Phys. Rev. Lett.* **79** 1738 (1998)
187. K Rathnayaka, A K Bhatnagar, A Parasiris, D Naugle, P C Canfield, B Cho *Phys. Rev. B* **55** 8506 (1997)
188. S V Shulga, S Drechsler, G Fuchs, K Muller, K Winzer, M Heinecke, K Krug *Phys. Rev. Lett.* **80** 1730 (1998)
189. M D Sumption, X Peng, E Lee, M Tomsic, E W Collings http://xxx.lanl.gov/abs/cond-mat/0102441 (2001)
190. G Grasso, A Malagoli, C Ferdeghini, S Roncallo, V Braccini, M R Cimberle, A S Siri *Appl. Phys. Lett.* **79** 230 (2001)
191. A Sharoni, O Millo, G Leitus, S Reich *J. Phys., Condens Matter* **13** L503 (2001)
192. C U Jung, J Choi, P Chowdhury, H P Kijoon, K Kim, M Park, H Kim, J Kim, Z Du, M Kim, W N Kang, S Lee, G Sung, J Y Lee http://xxx.lanl.gov/abs/cond-mat/0105330 (2001)
193. M Xu, H Kitazawa, Y Takano, J Ye, K Nishida, H Abe, A Matsushita, G Kido http://xxx.lanl.gov/abs/cond-mat/0105271 (2001)
194. J Hlinka, I Gregora, J Pokorny, A Plecenik, P Kus, L Satrapinsky, S Benacka http://xxx.lanl.gov/abs/cond-mat/0105275 (2001)
195. S Lee, H Mori, T Masui, Yu Eltsev, A Yamamoto, S Tajima http://xxx.lanl.gov/abs/cond-mat/0105545 (2001)
196. Appl. Russ. 108 865 (2001)
197. W N Kang, H Kim, E M Choi, C U Jung, S L Lee *Science* **292** 1521 (2001)
198. J H Jung, K W Kim, H J Lee, M W Kim, T W Noh, W N Kang, H Kim, E M Choi, C U Jung, S L Lee http://xxx.lanl.gov/abs/cond-mat/0105180 (2001)
199. S Patnaik, L D Cooley, A Gurevich, A A Polyanskii, J Jiang, X Y Cai, A A Squitieri, M T Naus, M K Lee, J H Choi, L Belenky, S D Bu, S D Letteri, X Song, D Schlom, S E Babcock, C B Eom, E E Hellstrom, D C Larbalestier *Supercond. Sci. Technol.* **14** 315 (2001)
200. H J Zhai, H M Christen, L Zhang, M Paranthaman, C Cantoni, B C Sales, P H Fleming, D K Christen, D H Lowndes http://xxx.lanl.gov/abs/cond-mat/0103618 (2001)
201. Z W Zhao, H H Wen, S L Li, Y M Ni, H P Yang, W N Kang, H J Kim, E M Choi, S I Lee http://xxx.lanl.gov/abs/cond-mat/0104249 (2001)
202. S F Wang, S Y Dai, Y I Zhou, Z H Chen, D F Cui, J D Yu, M He, H B Lu, G Y Yang *Chin. Phys. Lett.* **18** 967 (2001)
203. X D Zeng, A Sukiasyan, X X Xi, Y F Hu, E Wertz, Q Li, W Tian, H P Sun, X Pan, J Lettieri, D Schlom, C O Brubaker, Z Liu http://xxx.lanl.gov/abs/cond-mat/0105080 (2001)
204. A H Li, X L Wang, M Ionescu, S Soltonian, J Horvat, T Silver, H K Liu, S X Dou http://xxx.lanl.gov/abs/cond-mat/0104156 (2001)
205. H J Zhai, H M Christen, L Zhang, M Paranthaman, P H Fleming, D H Lowndes http://xxx.lanl.gov/abs/cond-mat/0104309 (2001)

206. S Y Lee, J H Lee, J S Ryu, J Lim, S H Moon, H N Lee, H G Kim, B Oh http://xxx.lanl.gov/abs/cond-mat/0105327 (2001)
207. H J Kim, W N Kang, F M Choi, M S Kim, K H P Kim, S I Lee http://xxx.lanl.gov/abs/cond-mat/0105363 (2001)
208. M H Jung, M Jaime, A H Lacerda, G S Boebinger, W N Kang, H J Kim, E M Choi, S I Lee http://xxx.lanl.gov/abs/cond-mat/0106146 (2001)
209. A Berenov, Z Lockman, X Qi, Y Bugoslavsky, L F Cohen, M H Jo, N A Stelmashenko, V N Tsaneva, M Cambara, N Hari Babu, D A Cardwell, M G Blamire, J L Mac Manus-Driscoll http://xxx.lanl.gov/abs/cond-mat/0106278 (2001)
210. C Ferdeghini, V Ferrando, G Grassano, W Ramadan, E Bellingeri, V Braccini, D Marre, P Manfrinetti, A Palenzona, F Borgatti, R Felici, T L Lee http://xxx.lanl.gov/abs/cond-mat/0107031 (2001)
211. V M Silkin, E V Chulkov, P M Echenique http://xxx.lanl.gov/abs/cond-mat/0105628 (2001)
212. Z Li, J Yang, J G Hou, Q Zhu http://xxx.lanl.gov/abs/cond-mat/0106590 (2001)
213. V A Gasparov, N I Sidorov, I I Zver'kova, M P Kulakov *JETP Lett*. **73** 532 (2001)
214. G K Strukova, V F Degtyareva, D V Shivkun, V N Zverev, V M Kiiko, A M Ionov, A N Chaika http://xxx.lanl.gov/abs/cond-mat/0105293 (2001)
215. D P Young, P W Adams, J Y Chan, F R Fronczek http://xxx.lanl.gov/abs/cond-mat/0104063 (2001)
216. T He, Q Huang, A P Ramirez, Y Wang, K A Regan, N Rogado, M A Hayward, M K Haas, J S Slusky, K Inumaru, H W Zandbergen, N P Ong, R J Cava *Nature (London)* **411** 6833 (2001)
217. A Taraphder, R Pandit, H R Krishnamurthy, T V Ramakrishnan *Int. J. Mod. Phys. B* **10** 863 (1998)
218. A L Ivanovskii *Usp. Khim*. **68** 119 (1999) [*Russ. Chem. Rev*. **68** 103 (1999)]
219. S Y Li, R Fan, X H Chen, C H Wang, W Q Mo, K Q Ruan, Y M Xiong, X G Luo, H T Zhang, L Li, Z Sun, L Z Cao http://xxx.lanl.gov/abs/cond-mat/0104554 (2001)
220. Z Q Mao, M M Rosario, R Nelson, K Wu, I G Deac, P Schiffer, Y Liu, T He, K A Regan, R J Cava http://xxx.lanl.gov/abs/cond-mat/0105280 (2001)
221. Q Huang, T He, K A Regan, N Rogado, M A Hayward, M K Haas, K Inumaru, R J Cava http://xxx.lanl.gov/abs/cond-mat/0105240 (2001)
222. M A Hayward, M K Haas, T He, K A Regan, N Rogado, K Inumaru, R J Cava http://xxx.lanl.gov/abs/cond-mat/0104541 (2001)
223. Z A Ren, G C Che, S L Jia, H Chen, Y M Ni, Z X Zhao http://xxx.lanl.gov/abs/cond-mat/0105366 (2001)
224. I R Shein, N I Medvedeva, A L Ivanovskii *JETP Lett*. **74** 122 (2001)
225. S B Dugdale, T Jarlborg http://xxx.lanl.gov/abs/cond-mat/0105349 (2001)
226. J H Shim, B I Min http://xxx.lanl.gov/abs/cond-mat/0105418 (2001)
227. D J Singh, I I Mazin http://xxx.lanl.gov/abs/cond-mat/0105577 (2001)
228. I R Shein, N I Medvedeva, A L Ivanovskii http://xxx.lanl.gov/abs/cond-mat/0107010 (2001)

[a] — *Russ. J. Gen. Chem. (Engl. Transl.)*
[b] — *Dokl. Chem. (Engl. Transl.)*
[c] — *Russ. J. Inorg. Chem. (Engl. Transl.)*
[d] — *Russ. J. Phys. Chem. (Engl. Transl.)*
[e] — *Inorg. Mater. (Engl. Transl.)*
[f] — *Phys. Solid State (Engl. Transl.)*
[g] — *Russ. J. Appl. Chem. (Engl. Transl.)*